In silico comparison of SARS-CoV-2 spike protein-ACE2 binding affinities across species and implications for viral origin

Sakshi Piplani[1,2], Puneet Kumar Singh[2], David A. Winkler[3-6]*, Nikolai Petrovsky[1,2]*

[1] College of Medicine and Public Health, Flinders University, Bedford Park 5046, Australia
[2] Vaxine Pty Ltd, 11 Walkley Avenue, Warradale 5046, Australia
[3] La Trobe University, Kingsbury Drive, Bundoora 3086, Australia
[4] Monash Institute of Pharmaceutical Sciences, Monash University, Parkville 3052, Australia
[5] School of Pharmacy, University of Nottingham, Nottingham NG7 2RD. UK
[6] CSIRO Data61, Pullenvale 4069, Australia

*Joint senior authors
Corresponding authors: –
Prof. Nikolai Petrovsky: nikolai.petrovsky@flinders.edu.au
Prof. Dave Winkler: d.winkler@latrobe.edu.au

Keywords: SARS-Cov-2; binding affinity; multiple species; angiotensin converting enzyme 2 (ACE2); spike protein (S protein); computational chemistry; docking and molecular dynamics.

Abstract

The devastating impact of the COVID-19 pandemic caused by SARS–coronavirus 2 (SARS-CoV-2) has raised important questions about viral origin, mechanisms of zoonotic transfer to humans, whether companion or commercial animals can act as reservoirs for infection, and why there are large variations in SARS-CoV-2 susceptibilities across animal species. Powerful *in silico* modelling methods can rapidly generate information on newly emerged pathogens to aid countermeasure development and predict future behaviours.

Here we report an *in silico* structural homology modelling, protein-protein docking, and molecular dynamics simulation study of the key infection initiating interaction between the spike protein of SARS-Cov-2 and its target, angiotensin converting enzyme 2 (ACE2) from multiple species. Human ACE2 has the strongest binding interaction, significantly greater than for any species proposed as source of the virus. Binding to pangolin ACE2 was the second strongest, possibly due to the SARS-CoV-2 spike receptor binding domain (RBD) being identical to pangolin CoV spike RDB. Except for snake, pangolin and bat for which permissiveness has not been tested, all those species in the upper half of the affinity range (human, monkey, hamster, dog, ferret) have been shown to be at least moderately permissive to SARS-CoV-2 infection, supporting a correlation between binding affinity and permissiveness. Our data indicates that the earliest isolates of SARS-CoV-2 were surprisingly well adapted to human ACE2, potentially explaining its rapid transmission.

Introduction

The devastating impact of COVID-19 infections caused by SARS–coronavirus 2 (SARS-CoV-2) has stimulated unprecedented international activity to discover effective vaccines and drugs for this and other pathogenic coronaviruses.[1-4] It has also raised important questions about the mechanisms of zoonotic transfer of viruses from animals to humans, whether companion animals or those used for commercial purposes can act as reservoirs for infection, and the reasons for the large variations in SARS-CoV-2 susceptibility across animal species.[5-7] Understanding how viruses move between species may help us prevent or minimize similar events in the future. Methods that elucidate the molecular basis for differences in species susceptibilities of may also shed light on why different human sub-groups exhibit differences in susceptibilities.[8]

The most important features of SARS-CoV-2 are its spike protein (S protein) and a functional polybasic cleavage site at the S1–S2 boundary.[9] The SARS-CoV-2 spike monomer consists of a fusion peptide, two heptad repeats, an intracellular domain, N-terminal domain, two subdomains and a transmembrane region.[10] The angiotensin converting enzyme 2 (ACE2) was identified as the main receptor for the SARS-CoV-2 S protein, as it is for SARS CoV, binding to which is a critical initiating event for infection. ACE2 is relatively ubiquitous in humans, existing in cell membranes in the lungs, arteries, heart, kidney, and intestines. It consists of an N-terminal peptidase M2 domain and a C-terminal collectrin renal amino acid transporter domain.

Non-human species vary markedly in their susceptibility to SARS-Cov-2[7,11,12] and their ACE2 receptor binding domains also differ substantially. The phylogenetic tree showing relatedness of ACE2 proteins across selected animal species is illustrated in Supplementary Figure 1. Several species, notably pangolin, bat and snake, have been postulated as a source or intermediate host for SARS-Cov-2.[11,13,14]

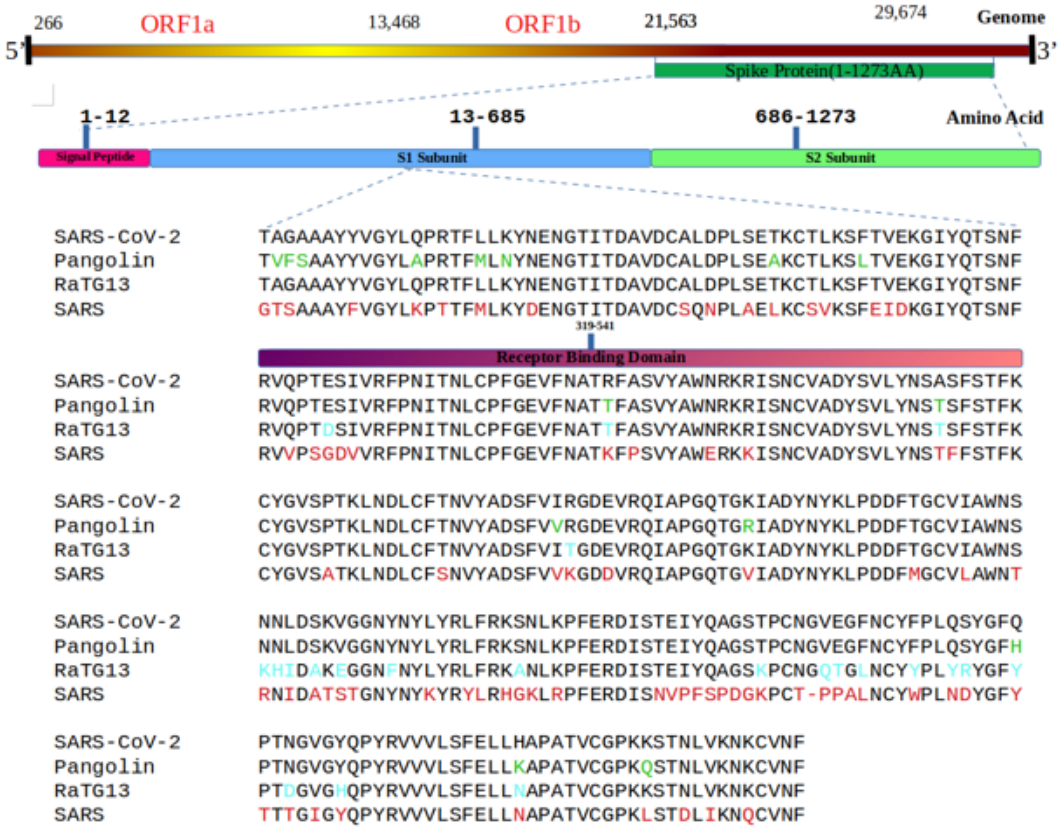

Figure 1. Sequence alignment of four closely related spike proteins. Difference in pangolin and bat spike proteins colored cyan and differences in SAR spike denoted in red. The receptor binding domain (RBD) is denoted by the red bar in the sequence alignments

We and others[15,16] postulate that variation in ACE2 structures between species will determine the binding strength of SARS-CoV-2 S protein and suggest which species are permissive to SARS-CoV-2 infection. For example, the low binding affinity of SARS S protein for mouse ACE2 has been postulated as the reason mice are largely non-permissive to SARS infection. Direct measurement of the binding affinity of SARS-CoV-2 S protein to ACE2 (e.g. using cell lines transfected with ACE2 proteins from different species) would be very useful but is time consuming, and purified or recombinant ACE2 proteins from all relevant animal species are not yet available.

Here we show how fast, efficient *in silico* structural modelling and docking algorithms from structure-based drug design can be used to determine the relative binding affinities of the SARS-CoV-2 S protein for ACE2, across multiple common and exotic animal species.[17-19] We provide novel insights into the species-specific nature of this interaction and impute which species might be permissive for SARS-CoV-2 that may help elucidate the origin of SARS-CoV-2 and the mechanisms for its zoonotic transmission.

Results and Discussion

The results of docking the receptor binding domains (RBDs) of SARS-CoV-2 S and ACE2 receptors of various species using the HDOCK server, refined by MD simulations, are summarized in Tables 1 and 2. The calculated binding energies for the interactions of SARS-CoV-2 with ACE2 from the species studied are summarized in Table 2, and the MMPBSA binding energies are listed for comparison. The energies calculated by equation 1 and those from the MMPBSA algorithm (see Materials and Methods) correlated strongly (r^2=0.76) but the energies correlated poorly with sequence similarity (r^2=0.27). The Kendall tau rank correlation for the two different methods of calculating binding energies was 0.94. Also shown is the observed and predicted SARS-CoV-2 susceptibilities of the species from analysis of phylogenetic clustering and sequence alignment with currently known ACE2s utilized by SARS-CoV-2, as described by Qiu et al.[20] (Supplementary Figure 4) For comparison, we show the interaction energies of the S and ACE2 proteins for each species calculated by Wu et al. using an automatic docking method, ICM-Pro[21] (no subsequent MD refinement), and observational *in vivo* data on SARS-CoV-2 infectivity and disease symptoms in the species, where this has been reported. The interaction energies calculated by Wu et al., based only on docking calculations, predict that monkey, hamster, tiger and bat have higher affinity than human ACE2 for the spike protein which is clearly not consistent with the known infectivities of the species in Table 2. This suggests that more sophisticated computational methods are required to obtain binding affinities more consistent with observation, as in the work presented here and by others, e.g.[22]

While this paper was being prepared, Rodrigues et al. published a similar study that used the docking method HADDOCK to estimate the relative strength of binding affinities of SARS-Cov-2 spike protein for ACE2 proteins of 30 species.[22] The docking experiments were followed by short MD simulations. This study found 18 species had higher affinity than the human ACE2, including dog, pangolin, ferret, Siberian tiger, horseshoe bat, civet, hamster and guinea pig but also goldfish, sheep, cat, horse and rabbit. Goldfish (no known permissiveness of infection with SARS-Cov-2) had the second highest affinity after dog. The authors stated that, despite their method having some discrimination between species that are susceptible and those that are not, their predictions were not entirely correct. For example, they rank guinea pig ACE2 (SARS-CoV-2 negative) as a better receptor for SARS-CoV-2 RBD than for human, cat, horse, or rabbit ACE2 (all SARS-CoV-2 positive species), despite experiments showing that there is negligible binding between the two proteins.[23] One

explanation may be that their MD simulations were short (simulation time not listed) and it longer simulations like those used in this study are needed to obtain more accurate ranking of the binding affinities.

Other relevant papers were also published while this paper was in preparation and review. Recently, Damas et al. published an analysis of ACE2 sequences from 410 vertebrate species, including 252 mammals, to study the probability that ACE2 could be used as a receptor by SARS-CoV-2.[15] They classed the species into five risk groups. Man, apes, and monkeys were in the very high-risk group while Chinese hamsters, whales and porpoises were prominent examples of species in the high-risk group.

Note added in proof: While this paper was undergoing review, a highly relevant paper was published in Scientific Reports (5 Oct) by Lam et al.[24] on the species specificity of spike-ACE2 interaction. This provides validation of our computational approach and results we obtained on the relative binding affinities of non-human species. As with our study they used MODELLER to generate ACE2 structures for difference species and selected the best refined model using DOPE scores. They calculated free energy differences, $\Delta\Delta G$, between human ACE2 binding and that of non-human species ACE2 to SARS-Cov-2 spike using free energy perturbation methods. However, energy differences they calculated are similar to those we calculated. Unfortunately, Lam et al. did not report the $\Delta\Delta G$ for the most important species, pangolin, making our study significant in reporting this binding energy.

Table 1. ACE2 RBD residues interacting with the S protein RBD from MD simulations of complexes. Residues interacting with the same S residue in different species ACE2, that differ from those in human ACE2, are labelled green (conservative replacements) or red (non-conservative replacements).

Species	Accession Number	Position																% common residues
		19	24	27	28	30	31	34	37	38	41	42	79	83	330	353	393	
Homo sapiens (human)	Q9BYF1	S	Q	T	F	D	K	H	E	D	Y	Q	L	Y	N	K	R	100
Macaca fascicularis (monkey)	A0A2K5X283	S	Q	T	F	D	K	H	E	D	Y	Q	L	Y	N	K	R	100
Panthera tigris (tiger)	XP_007090142.1	S	L	T	F	D	K	H	E	**E**	Y	Q	L	Y	K	K	R	94
Bos Taurus (cow)	NP_001019673.2	S	Q	T	F	**E**	K	H	E	D	Y	Q	**M**	Y	N	K	R	88
Mesocricetus auratus (hamster)	A0A1U7QTA1	S	Q	T	F	D	**L**	**Q**	E	D	Y	Q	L	Y	N	K	R	88
Felis catus (cat)	Q56H28	S	**L**	T	F	**E**	K	H	E	**E**	Y	Q	L	Y	N	K	R	81
Rhinolophus sinicus (bat)	U5WHY8	S	**E**	**M**	F	D	K	**T**	E	D	**H**	Q	L	Y	N	K	R	75

Species	Accession Number	Position																% common residues
		19	24	27	28	30	31	34	37	38	41	42	79	83	330	353	393	
Homo sapiens (human)	Q9BYF1	S	Q	T	F	D	K	H	E	D	Y	Q	L	Y	N	K	R	100
Paguma larvata (civet)	Q56NL1	S	L	T	F	E	K	Y	E	Q	Y	Q	L	Y	N	K	R	75
Equus ferus caballus (horse)	F6V9L3	S	L	T	F	D	K	S	E	E	H	Q	L	Y	N	K	R	75
Mustela putorius furo (ferret)	Q2WG88	D	L	T	F	E	K	T	E	E	Y	Q	-	Y	N	K	R	69
Canis luparis (dog)	J9P7Y2	-	L	T	F	E	K	Y	E	E	Y	Q	L	Y	N	K	R	69
Mus musculus (mouse)	Q8R0I0	S	N	T	F	N	N	Q	E	D	Y	Q	Y	F	N	K	R	63
Manis javanica (pangolin)	XP_017505752.1	-	E	T	F	E	K	S	E	E	Y	Q	I	Y	N	K	R	63
Ophiophagus Hannah (snake)	ETE61880.1	Q	V	K	F	E	Q	A	-	D	Y	N	N	F	N	L	R	38

Table 2. Binding energies of SARS-Cov-2 spike to ACE2 for different species and potential species susceptibilities from other studies

Species	E_{eqn1} (kcal/mol)	E_{MMPBSA} (kcal/mol)	SARS-Cov-2 infectivity	Binding score Wu et al.[21]	ACE2 used by SAR-Cov-2 spike[20]
Homo sapiens (human)	-52.8	-57.6 ± 0.25	Permissive, high infectivity, severe disease in 5-10%,	-50.1	confirmed
Manis javanica (pangolin)	-52.0	-56.3 ± 0.4	Permissive [25,26]	-46.4	predicted
Canis luparis (dog)	-50.8	-49.5	Permissive, low/mod infectivity, no overt disease [27,28]	-40.7	predicted
Macaca fascicularis (monkey)	-50.4	-50.8	Permissive, high infectivity, lung disease [11]	-51.5	
Mesocricetus auratus (hamster)	-49.7	-50.0	Permissive, high infectivity, lung disease [29,30]	-50.4	
Mustela putorius furo (ferret)	-48.6	-49.2	Permissive, moderate infectivity, no overt disease [30-32]	-45.4	
Felis catus (cat)	-47.6	-48.9	Permissive, high infectivity, lung disease [28,31,33]	-48.9	predicted
Panthera tigris (tiger)	-47.3	-42.5	Permissive, overt disease, RNA positive[28]	-50.6	
Rhinolophus sinicus (bat)	-46.9	-50.1 ± 1.0	Permissive? No reported infections [11]	-50.4	confirmed
Paguma larvata (civet)	-45.1	-46.1	No reported infection	-49.4	confirmed
Equus ferus caballus (horse)	-44.1	-49.2	No naturally occurring infections[28]	-48.0	predicted
Bos taurus (cattle)	-43.6	-42.5	No naturally occurring infections[28]		predicted
Ophiophagus hannah (king cobra)	-39.5	-40.7 ± 1.2	No reported infection	-45.4	
Mus musculus (mouse)	-38.8	-39.4	Resistant to infection[30]	-44.7	confirmed not used

Golden hamsters, cattle and cats were members of the medium risk group and dogs, horses and bats were in the low risk group. Pangolins, ferrets, mice, and minks were assigned to the very low risk group in their analyses. The susceptibility predictions from these studies also do not correlate well with observations, consist with the low correlation between binding energies and sequence noted above.

Two additional, recent studies have some relevant to our study. Spinello et al. published a detailed, microsecond molecular dynamics simulation of the key molecular interactions driving the higher affinity/specificity of SARS-CoV-2 toward ACE2 as compared to SARS-CoV.[34] However, this study did not compare the affinities of non-human ACE2 proteins for the SARS-Cov-2 spike protein. Subsequently, Wang and co-workers published a complementary MD study comparing the interactions of SARS-Cov-2 and SARS-Cov spike proteins with the human ACE2 protein with 200 ns simulations.[35] They analysed the receptor binding of SARS-CoV-2 in terms of key electrostatic interactions, networks of hydrogen-bonding and hydrophobic interactions in the RBD. Again, no other species were considered in the study.

The key interacting residues of ACE2 receptor and SARS-CoV-2 S protein (Table 1) were broadly consistent with these previous studies [34-36]. Conserved amino acids in ACE2 of most species were largely those interacting with the S protein. PHE28, ASN330, ASP355 and ARG357 were conserved in all the species and all interacted with the spike protein. TYR41, LYS353, ALA386 and ARG393 were conserved and interacting in all species except bat, mouse, ferret and pangolin. Residues interacting with the S protein in ACE2 from *Ophiophagus hannah* (King cobra) were least conserved, consistent with its low sequence similarity to human ACE2.

Computed binding affinities suggest that SARS-Cov-2 S protein is optimized for human ACE2

Identifying species permissive to SARS-CoV-2 is very important for identifying intermediate hosts and potential source of the original virus, and for developing infection models for testing of COVID-19 drugs and vaccines. SARS-CoV-2 traces back to the human, civet, and bat SARS CoV strains, all of which use the ACE2 protein of each relevant species for cellular entry.[37-39] The SARS-CoV-2 and SARS CoV sequences have only 72% identity in the RBD regions showing they are only distantly related, even though they bind the same ACE2 receptor. The closest coronavirus to SARS-CoV-2 identified to date is the bat CoV, RaTG13, but it has a different spike protein that lacks the polybasic furin cleavage site and uses a different RBD. The RBD of pangolin CoV is most similar to that of SARS-CoV-2, meaning that much of early interpretation of the ancestry of SARS-CoV-2 was based on this sequence analysis (Figure 1).

Our structure-based approach revealed some surprisingly results, contrasting with to those from sequence based analyses. Conspicuously, the predicted binding between SARS-CoV-2 S protein

and ACE2 was strongest overall for humans than for any species studied. The predicted strength of SARS-CoV-2 S protein binding to ACE2 being human > pangolin > dog > monkey > hamster > ferret > cat> tiger > bat > civet > horse > cow > snake > mouse ACE2.

Spike protein mutations are rare, especially in the receptor binding domain (RBD) that interacts with ACE2. For the SARS-Cov-2 S protein, only three mutational sites, V367F, G476S, and V483A, have been identified within the RBD domain. Of these, only G476S occurs directly at the binding interface of RBD and the peptidase domain of ACE2 and its incidence and geographic spread is very small.[40] This minimal mutation in the spike RBD during the history of the pandemic suggests that the spike RBD was already optimally adapted to bind human ACE2. This finding is surprising as, typically, a virus exhibits the highest affinity for receptors in its original host species, presumed by most to be bat, with a lower initial affinity for the receptor of any new host species such as humans. Then as the virus mutates and adapts to its new host species, the binding affinity might be expected to increase over time. Since our calculations are based on SARS-Cov-2 S sequences samples isolated in December and hence from very early in the outbreak, the finding that the affinity of SARS-CoV-2 S protein is higher for human ACE2 than for any other putative host species was unexpected.

This very high affinity for human ACE2 was confirmed very recently (July 10) in a preprint by Alexander et al.[41] who also studied the RBD of spike-ACE2 for several species and reported that the SARS-CoV-2 RBD sequence is optimal for binding to human ACE2 compared to other species. They also described this as a remarkable finding that underlies the high transmissibility of the SAR-Cov-2 virus amongst humans. These results are also consistent with a recent report comparing SARS-CoV and SARS-CoV-2 that found a number of differences in the SARS-CoV-2 RBD that made it a much more potent binder to human ACE2 through the introduction of numerous hydrogen bonding and hydrophobic networks[35] helping explain the efficient and rapid transmission SARS-CoV-2 through the human population, once a presumed cross-over event occurred in or around November 2019.

Interestingly, as shown in Table 1, pangolin and human ACE2 are closest in binding energy despite being structurally different and only sharing 10 of 16 interacting residues at the SARS-CoV-2 RBD. This similarity of binding energy is interesting as pangolins have previously been imputed as a potential intermediate host to explain the spill-over of a putative bat coronavirus to humans. However, most of the pangolin ACE2 RBD differences are conservative replacements of residues in the human ACE2 RBD viz. Q24E, D30E, D38E, L79I that are likely to make similar contributions to the binding interaction with SARS-CoV-2 spike. The main differences are the lack of S19 interaction and the replacement of H34 by S34 in pangolin ACE2. However, the MD structures

show that the OH moiety in the sidechain of S24 lies in the same region, and can make similar interactions, as the NH moiety in the imidazole sidechain of H34.

Affinity of ACE2 from non-human species

SARS-CoV-2 also recognizes ACE2 from a variety of animal species, including palm civet, the intermediate host for SARS-CoV.[42] The calculated binding energies of SAR-CoV-2 S protein with ACE2 from other species is in general agreement with the relatively limited amount of published information on species infectivity. Predicted binding to monkey ACE2 is 2.4 kcal/mol lower than for human ACE2, despite all 16 ACE2 binding residues being the same This relatively small binding energy difference appears to reside in structural changes outside the RBD. Several studies have reported the susceptibility of various animal species to SARS-CoV-2[5,43,44] with susceptible species such as macaques, hamsters and ferrets used as animal models of SARS-CoV-2 infection.[29,45,46]

Infected young cynomolgus macaques expressed viral RNA in nasal swabs but did not develop overt clinical symptoms, whereas aged animals showed higher viral RNA loads, some weight loss, and rapid respiration associated with moderate interstitial pneumonia and virus replication in upper and lower respiratory tract.[46,47] Hamster ACE2 had a high predicted binding to the S protein, similar to that for monkey ACE2, with hamster ACE2 sharing 14 out of 16 binding residues with human ACE2. The model predicts that hamster should be permissive to SARS-CoV-2 infection based on the strong binding of SARS-Cov-2 S protein for hamster ACE2 (Table 2). Syrian hamsters have been shown to exhibit clinical and histopathological responses to SARS-CoV-2 that closely mimic human upper and lower respiratory tract infections, with high virus shedding and ability to transmit to naïve contact animals, [29] consistent with the model predictions. This high susceptibility to SARS-CoV infection of Syrian hamsters makes them one of the best animal models of infection. Ferrets are also permissive to SARS CoV infection, and our modelling data indicated that SARS-CoV-2 has a similar binding energy to ferret and hamster ACE2 (Table 2). Consistent with our model data, ferrets are permissive to infection with SARS-CoV-2, with high virus titre in the upper respiratory tract, virus shedding, infected ferrets showing acute bronchiolitis although without severe disease or death, and active transmission to naïve ferrets through direct contact.[44,45]

There is inefficient virus replication of SARS-CoV or SARS-CoV-2 in mice making them unsuitable as models to test SARS or COVID-19 vaccines or drugs. [48] Mice only became permissive for SARS infection when made transgenic for human ACE2 e.g. Golden et al. recently reported that transgenic mice expressing human ACE2 become highly susceptible to SARS-CoV-2.[49] Cat and tiger ACE2 were shown by our model to have similar binding affinity for SARS-CoV-2 S protein and both these species have been shown to be permissive for SARS-CoV-2 infection.

Similarly, our data suggests that SARS-CoV-2 binds with relatively high affinity to dog ACE2 suggesting that dogs may be susceptible to infection. In the case of companion animals that live in close proximity to humans, Shen at al. found that that SARS-CoV-2 could be efficiently transmitted in cats and dogs [50] while Shi et al. reported that SARS-CoV-2 replicates poorly in dogs, pigs, chickens, and ducks, but that ferrets and cats were permissive to infection.[31] Temmam et al. tested 9 cats and 12 dogs living in close contact with their owners, two of whom tested positive for SARS-CoV-2 and 11 of 18 others showed clinical signs of COVID-19 but no antibodies against SARS-CoV-2 were detectable in their blood using an immunoprecipitation assay.[51] Goumeniu et al. published an editorial querying the role of dogs in the Lombardy COVID-19 outbreak and recommended use of computational docking experiments to provide evidence for, or against infection of dogs.[52] Our model data suggesting that dog ACE2 might be permissive for SARS-CoV-2 binding and infection is therefore consistent with anecdotal reports of dogs being infected with SARS-CoV-2. Genetic and other factors could underlie the apparent inconsistent reporting of susceptibility of dogs to COVID-19 clinical infection.

Implications for the intermediate animal vector for SARS-Cov-2

Bats have been suggested as the original host species of SARS-Cov-2 infections in humans, with pangolins acting as an intermediate animal vector. Bat CoV RaTG13 has the highest sequence similarity to SARS-CoV-2, with 96% whole-genome identity (50)., but does not possess neither the furin cleavage site or the pangolin RBD seen in SARS-CoV-2. Could SARS-CoV-2 be an as-yet unidentified bat virus? Although bats carry many coronaviruses, no evidence of a direct relative of SARS-CoV-2 in bat populations has so far been found. As highlighted by our data, the binding affinity of SARS-CoV-2 for bat ACE2 is considerably lower than for human ACE2 and human ACE2 has been shown to not to bind the RaTG13 spike [53]. This suggests that even if SARS-CoV-2 did originally arise from a bat precursor, it must have spent considerable time in another host wherein it adapted its S protein to bind better to the host ACE2. This also resulted in acquiring higher affinity for human ACE2 while lowering its affinity to the original bat ACE2. There are currently no known explanations for how or where this transition to generate the ultimate SARS-CoV-2 spike protein could have occurred. Evidence of direct human infection by bat coronaviruses or other viruses is rare, with transmission typically involving an intermediate host. For example, SARS-CoV was shown to be transmitted from bats to civet cats and then to humans. The S protein must acquire new mutations to enable this transition to occur, first to increase its affinity for civet ACE2 and then to increase its affinity for human ACE2. To date, a virus directly related to SARS-CoV-2 has not been identified in bats or any other non-human species, making its origins unclear. Moreover, Wrobel et al. reported a structural biology study of the bat virus and SARS-Cov-2 and

reported the experimental binding affinities of human ACE2 for the S proteins of these viruses.[53] They concluded that, although the structures of human SARS-CoV-2 and bat RaTG13 S proteins are similar, the human S protein has a more stable pre-cleavage form, and the human ACE2 binding k_D was 68±9 nM while RaTG13 bound human ACE2 with a k_D >40 μM. They observed that cleavage at the furin-cleavage site decreases the overall stability of SARS-CoV-2 S protein and fosters the open conformation required for S to bind to the ACE2 receptor. They concluded that their data indicate that a bat virus would not bind effectively to human ACE2 receptor and would be unlikely to infect humans. Early in the COVID-19 outbreak it was suggested that snakes may also be an intermediate vector. ACE2 of turtle and snake has very low homology to human ACE2 and SARS-CoV-2 was shown not to bind to reptile ACE2, making snakes unlikely intermediate hosts for SARS-CoV-2. [14]

The pangolin ACE2, despite having lower sequence similarity to human ACE2 (86%) than other tested species (e,g. monkey ACE2 - 97% similarity to human), had the most similar binding affinity to that of human ACE2. However, the predicted binding strength of SARS-CoV-2 S protein to pangolin ACE2 was lower than to human ACE2, with the difference being highly significant (two-tailed p = 0.0013). All other binding affinities were substantially lower then human and pangolin ACE2 and were significant at the >>99.99% confidence level. It was reported recently that a coronavirus isolated from Malayan pangolins shared the same RDB sequence as SARS-CoV-2, which raised the possibility that pangolins may have acted as the intermediate vector between bats and humans. Although it has the same spike RBD as SARS-CoV-2, pangolin-CoV is not closely related to SARS-CoV-2 overall, with <90% sequence similarity across its whole genome. [25] It is noteworthy that the common spike RBD in both pangolin CoV and SARS-CoV-2 is able to bind strongly to both pangolin and human ACE2, despite significant differences in the sequences of the ACE2 RDB (only 63% of residues are common (Table 1)). Xiao reported a pangolin-CoV that has 100%, 98.6%, 97.8% and 90.7% amino acid identity with SARS-CoV-2 in the E, M, N and S proteins.[26] They surprisingly reported the RBD of the pangolin S protein to be almost identical to that of SARS-CoV-2 despite 4 of the 10 residues interacting with ACE2 being different viz. H34S, L79I, M82N and G354H. They suggested pangolins as potential intermediate hosts of SARS-CoV-2. Additionally, pangolin CoV isolated from Malayan pangolins from two different regions in China showed differences in the residues interacting with human ACE2.[25] Pangolin-CoV was detected in 17 out of the 25 infected Malayan pangolins that that showed clinical signs and histological changes, and had antibodies against pangolin-CoV that also recognised the S protein of SARS-CoV-2. Another origin possibility might be that a pangolin was simultaneously co-infected with a bat ancestor to SARS-CoV-2 and a pangolin CoV. This could allow a recombination event to occur whereby the spike RBD of the pangolin virus was inserted into the bat CoV, thereby conferring the

bat CoV with high binding for both pangolin and human ACE2. Such recombination events are known to occur with other RNA viruses and can explain creation of some pandemic influenza strains[54]. Nevertheless, such events are by necessity rare as they require coinfection of the one host at exactly the same time. Most importantly, if such a recombination event had occurred in pangolins it would be expected to have similarly triggered an epidemic spread of the new highly permissive SARS-CoV-2-like virus among pangolin populations, such as we now see occurring across the human population. Currently there is no evidence of such a widespread pangolin SARS-CoV-2 like outbreak, making this scenario less likely. Of course, some pangolins might have been protected from SARS-CoV-2 infection by the existence of neutralising antibodies cross-protective against both pangolin CoV and SARS-CoV-2, given their close RBD similarity. Notably, all pangolin coronaviruses identified so far lack the furin-like S1/S2 cleavage site in the SARS-CoV-2 spike protein that facilitates its rapid spread through human populations.

The high affinity of SARS-CoV-2 S protein for human ACE2 may be explicable if a recombination event took place in the past between a SARS-CoV-2 progenitor virus and pangolin CoV that resulted in insertion of the pangolin CoV RBD into the SARS-CoV-2 genome. However, the SARS-CoV-2 genome was recently reported to exhibit no evidence of recent recombination, arguing against this possibility.[55] Also, as he pangolin-CoV S protein does not have the furin cleavage site that is a prominent feature of the SARS-CoV-2 S protein,[51] this argues against pangolins being the intermediate vector for transmission of SARS-CoV-2 to humans. The major similarity of SARS-CoV-2 to pangolin-CoV lies in the RBD residues in the S protein that SARS-CoV-2 acquired by some unknown mechanism. As coronaviruses from nonhuman species with similar ACE2 receptors have not been sampled extensively, it is possible that a direct or intermediate animal source has yet to be found. This would preclude identification of evolutionary changes immediately prior to or during the jump to humans.

Gain of function (GoF) mutations occur in viruses that can lead to pandemics. For example, GoF mutations in influenza virus are associated with mammalian transmissibility, increased virulence for humans, and evasion of existing host immunity.[54] The conditioning of viruses to humans as pandemics progress is well recognized. Phylodynamic analyses of the COVID-19 genomes estimated the date for the most recent common ancestor from the start to middle of December, consistent with the earliest reported date 1st December 2019 for the initial cluster of pneumonia cases.[56] This study concluded, based on available genome sequence data, that the current epidemic has been driven entirely by human to human transmission at least since December. As the SARS-CoV-2 structure that we employed was obtained from viruses collected early in the outbreak, it is not clear how these early strains of SARS-CoV-2 developed such a high affinity for human ACE2. This suggests that SARS-CoV-2 spike RBD previously evolved by selection on a

human-like ACE2. Notably, pangolin ACE2 bears major differences in its RBD to human ACE2. Therefore its is surprising that pangolin-CoV has a similar RBD to SARS-CoV-2 that forms the basis for implicating pangolins directly or indirectly in the origins of SARS-CoV-2. The fact that pangolin CoVs can use human ACE2 for cell entry suggests that pangolin CoVs could represent a source of future human coronavirus pandemics if they were to gain the SARS-CoV-2 furin cleavage site.

Given the seriousness of the ongoing SARS-CoV-2 pandemic, it is imperative that all efforts be made to identify the original source of the virus. One question to be addressed is whether the virus is completely natural and was transmitted to humans by an intermediate animal vector, or whether it came from a recombination event that occurred inadvertently or intentionally in a laboratory handling coronaviruses, with the new virus being inadvertently released into the local human population. This is of key importance given the ability to use such information to help prevent any similar outbreak in the future. The one positive to our observation that SARS-CoV-2 already has optimised high binding to human ACE2, providing little selective pressure for mutations in the spike RBD to further increase binding affinity. Thus, a vaccine that induces neutralising antibody to the spike RBD may remain effective long-term, and not need to be modified regularly like influenza vaccines to keep up with RBD mutations.

Materials and Methods

Homology modelling of S protein and ACE2 from multiple species. As no three-dimensional structure of the SARS-CoV-2 S protein was available at the commencement of the project, we generated a homology structure the sequence retrieved from NCBI Genbank Database (accession number YP_009724390.1) in January 2020. A PSI-BLAST search against the PDB database for template selection was performed and the x-ray structure of SARS coronavirus S template (PDB ID 5XLR) was selected with 76.4% sequence similarity to SARS-CoV-2 S protein. The sequence alignment and sequences of related bat and pangolin coronaviruses are shown in Figure 1.

The protein sequences of the ACE2 proteins for different species and full sequence alignment in are shown in Supplementary Figure 2. The phylogenetic tree for ACE2 proteins from selected animal species is illustrated in Supplementary Figure 1. Protein preparation and removal of non-essential and non-bridging water molecules for docking studies and analysis of docked proteins was performed using the UCSF Chimera package (https://www.cgl.ucsf.edu/chimera/).[57]

The 3D-structures of the RBD of SARS-Cov-2 S and non-human ACE2 proteins were built using Modeller 9.23 (https://salilab.org/modeller/)[58] using the SARS S protein template to generate the homology model of SARS-Cov-2 S. The ACE2 receptors of selected species were similarly homology modelled using the following template structures – 1R42 (human ACE2), 3CSI (human glutathione transferase) and 3D0G (ACE2 structure from spike protein receptor-binding domain from the 2002-2003 SARS coronavirus human strain complexed with human-civet chimeric receptor ACE2) (Supplementary Table 1). Template similarity is important for model building the model; the sequence of *Macaca fascicularis* (monkey, accession number A0A2K5X283) was 97%

similar to that of human ACE2 while *Ophiophagus hannah* (king cobra) had a much lower similarity of 61% this template. The quality of the generated models was evaluated using the GA341 score [59] and DOPE ((Discrete Optimized Protein Energy) method scores[60], and the models assessed using SWISS-MODEL structure assessment server (https://swissmodel.expasy.org/assess).[61] Structures with the lowest DOPE score were refined by MD simulations (*vide infra*) and used for further analysis.

The modelled structures were also assessed for quality control using Ramachandran Plot and molprobity scores in SWISSModel. The Ramachandran plot checks the stereochemical quality of a protein by analysing residue-by-residue geometry and overall structure geometry and visualizing energetically allowed regions for backbone dihedral angles ψ against φ of amino acid residues in protein structure. The Ramachandran score of SARS-CoV-2 spike protein was 90% in the binding region and the molprobity score was 3.17. The Ramachandran score of the percentage of amino acid residues in the various species ACE2 that fall into the energetically favoured region ranged from 96-99% (Supplementary Table 2). The predicted ACE2 structures and Ramachandran plots for each species are summarized in Supplementary Figure 3. The molprobity provides evaluation of model quality at both the global and local level, this combines protein quality score that reflects the crystallographic resolution of a model.[62] It is a log-weighted combination of the number of serious atom clashes per 1000 atoms, percentage Ramachandran not favoured, and percentage bad side-chain rotamers. A good molprobity score is one that is equal to or lower than the crystallographic resolution. For reference, the MolProbity score for the x-ray structures of the templates (PDB IDs) were: 1R42= 3.01; 3SCI=3.14; 3D0G=2.74 and 6M17=1.99. The Ramachandran and Molprobity scores show that all the built structures were of good quality and suitable for use in further studies.

The structure of the SARS-Cov-2 S protein was published subsequently (e.g. PDB ID 6VXX and 6VYB). [63] Figure 2 shows the very high structural similarity of our homology modelled spike protein structure with the EM structures (PDB ID 6LZG (RBD) and 6VYB (open state)) with RMSD of 0.36 Å.

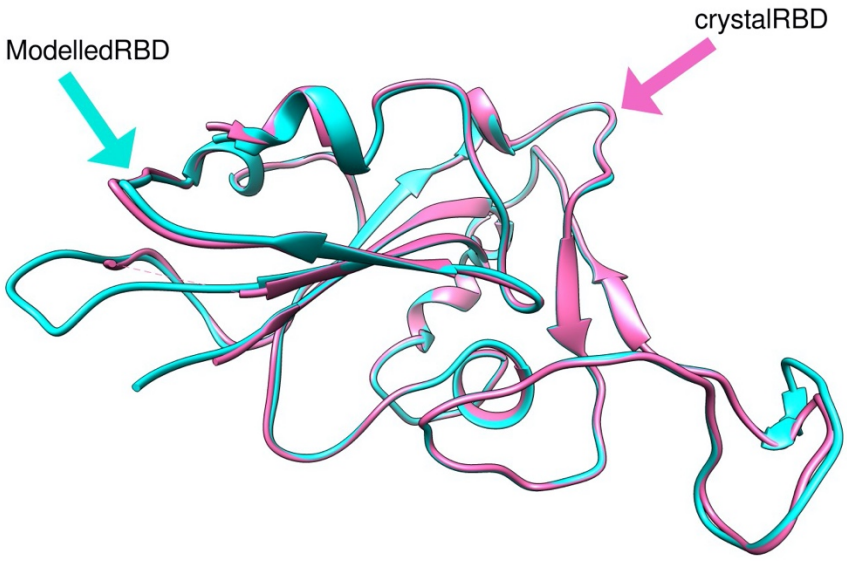

Figure 2. 3D structure of SARS-CoV-2 S protein (PDB PDB ID 6VYB (open form) and the homology modelled structure from Modeller

Docking of SARS-Cov-2 S protein with ACE2 proteins. These homology modelled ACE2 structures were docked against SARS-CoV-2 S protein structure using a state-of-the-art package HDOCK (http://hdock.phys.hust.edu.cn/).[64,65] This performs rigid-body docking by mapping the receptor and ligand molecules onto grids. Molecular docking was performed on the homology modelled SARS-CoV-2 S protein and human and animal ACE2 proteins using the hybrid docking method because attempts to use the template-free docking method with the structures generated by Modeller were unsatisfactory. The hybrid method used the structural template for the complex (PDB ID 6M17) to generate the results reported here. All docking poses were ranked using an energy-based scoring function.

The hybrid docking procedure may potentially introduce bias into the structures of the S protein bound to ACE2 from non-human species because it uses a human ACE2 complex x-ray structure as a template. To check for possible bias, the ACE2 structures generated by HDOCK were compared with those generated independently by Modeller. The Cα backbones of the ACE2 structures aligned with RMSD values between 0.5-0.8 Å (see Supplementary Table 3), exhibiting very strong structural similarities. Additionally, complexes were subjected to molecular dynamics simulation to wash out any template-induced bias.

Molecular dynamics simulation of docked complexes. The final docked SARS-Cov-2 spike/ACE2 protein complexes were optimized using the AMBER99SB-ILDN force field in GROMACS2020 (http://www.gromacs.org/).[66] Simulations were carried out using the GPU accelerated version of the program with the AMBER99SB-ILDN force field and implementing periodic boundary conditions in ORACLE server. Docked complexes were immersed in a truncated octahedron box of TIP3P water molecules. The solvated box was further neutralized with Na+ or Cl− counter ions using the tleap program. Particle Mesh Ewald (PME) was employed to calculate the long-range electrostatic interactions. The cut-off distance for the long-range van der Waals (VDW) energy term was 12.0 Å. The system was minimized without restraints. We applied 2500 cycles of steepest descent minimization followed by 5000 cycles of conjugate gradient minimization. After system optimization, the MD simulations was initiated by gradually heating each system in the NVT ensemble from 0 to 300 K for 50 ps using a Langevin thermostat with a coupling coefficient of 1.0/ps and with a force constant of 2.0 kcal/mol·Å2 on the complex. Finally, a production run of 100 ns of MD simulation was performed under a constant temperature of 300 K in the NPT ensemble with periodic boundary conditions for each system. During the MD procedure, the SHAKE algorithm was applied to all covalent bonds involving hydrogen atoms. The time step was 2 fs. The structural stability of the complex was monitored by the RMSD and RMSF values of the backbone atoms of the entire protein. Finally, the free energies of binding were calculated for all simulated docked structures.

Calculations were also performed for up to 500 ns on human ACE2 to ensure that 100ns is sufficiently long for convergence. Multiple production runs with different starting random seeds were used to estimate binding energy uncertainties for the strongest binding ACE2 structures – human, bat, and pangolin. All complexes stabilized during simulation with RMSD fluctuations converging to a range of 0.5 to 0.8 nm. The RMSD values for superimposition of the Cα backbones of each ACE2 structure before and after 100ns simulation was 1.2±0.1 Å, showing significant movement away from the initial HDOCK structures.

We found that the complex had stabilised after 50ns so considered that 100ns was an adequate simulation time. We also compared 100ns simulated structures of the ACE2 proteins from all species against those generated by homology modelling (most x-ray structures were not available) and found the RMSD values for Cα alignments

between 0.5-0.8 Å. This suggests that any memory of the human template has been removed or minimized. We also compared the structures generated independently by homology (Modeller) and HDOCK (Supplementary Table 3) and they agreed very well (RMSD< 1Å)

Calculation of binding free energies of complexes. The binding free energies of the protein-protein complexes were evaluated in two ways. The traditional method is to calculate the energies of solvated SARS-CoV-2 S and ACE2 proteins and that of the bound complex proteins and derive the binding energy by subtraction.

$$\Delta G \text{ (binding, aq)} = G \text{ (complex, aq)} - G \text{ (spike, aq)} - G \text{ (ACE2, aq)} \quad (1)$$

We also calculated binding energies using the molecular mechanics Poisson Boltzmann surface area (MM-PBSA) tool in GROMACS that is derived from the nonbonded interaction energies of the complex.[67,68] The method is also widely used method for binding free energy calculations. The binding free energies of the protein complexes were analysed during equilibrium phase from the output files of 100 ns MD simulations. The `g_mmpbsa` tool in GROMACS was used after molecular dynamics simulations, the output files obtained were used to post-process binding free energies by the single-trajectory MM-PBSA method. Specifically, for a non-covalent binding interaction in the aqueous phase the binding free energy,

$$\Delta G \text{ (bind,aqu)} = \Delta G \text{ (bind,vac)} + \Delta G \text{ (bind,solv)} \quad (2)$$

where ΔG (bind,vac) is the binding free energy in vacuum, and ΔG(bind,solv) is the solvation free energy change upon binding: –

$$\Delta G \text{ (bind,solv)} = G \text{ (R:L, solv)} - G \text{ (R,solv)} - G \text{ (L,solv)} \quad (3)$$

where G (R:L,solv), G (R,solv) and G (L,solv) are solvation free energies of complex, receptor and ligand, respectively.[69]

Free energy decomposition analyses were also performed by MM-PBSA decomposition to get a detailed insight into the interactions between the ligand and each residue in the binding site. The binding interaction of each ligand–residue pair includes three terms: the van der Waals contribution, the electrostatic contribution, and the solvation contribution.

As the simulations are very lengthy, we only ran multiple simulations for the species proposed as intermediate hosts and potential sources of the original virus, human, pangolin, bat and snake to estimate the uncertainty in the binding energies. As the ACE2 proteins for all species were extremely similar, we expected that these simulation error estimates would be of the same order for all other species. The predicted binding energies for these other species were significantly lower than those of human ACE2. We also used a statistical test to calculate the probability of the pangolin and human ACE2 affinities being different.

Data Availability. The coordinates of the S protein-ACE2 complexes will be deposited in. data repositories at La Trobe University and Flinders University.

ACKNOWLEDGEMENTS

We would like to thank Harinda Rajapaksha for assistance to optimise GROMACS for this project. We would also like to thank Oracle for providing their Cloud computing resources for the modelling studies described herein. In particular, we wish to thank Peter Winn, Dennis Ward, and

Alison Derbenwick Miller from Oracle in facilitating these studies. The opinions expressed herein are solely those of the individual authors and should not be inferred to reflect the views of their affiliated institutions, funding bodies or Oracle corporation.

Author contributions

Petrovsky - conceived project, analysed data, contributed to manuscript; Piplani and Singh - performed the computations, analysed data, contributed to the manuscript; Winkler - analysed data and contributed to manuscript

References

1 Berkley, S. COVID-19 needs a big science approach. *Science* **367**, 1407, doi:10.1126/science.abb8654 (2020).

2 Sanders, J. M., Monogue, M. L., Jodlowski, T. Z. & Cutrell, J. B. Pharmacologic Treatments for Coronavirus Disease 2019 (COVID-19): A Review. *J. Am. Med. Assoc.* **323**, 1824-1836, doi:10.1001/jama.2020.6019 (2020).

3 Sohrabi, C. *et al.* World Health Organization declares global emergency: A review of the 2019 novel coronavirus (COVID-19). *Int. J. Surg.* **76**, 71-76, doi:10.1016/j.ijsu.2020.02.034 (2020).

4 Thanh Le, T. *et al.* The COVID-19 vaccine development landscape. *Nat. Rev. Drug Discov.* **19**, 305-306, doi:10.1038/d41573-020-00073-5 (2020).

5 Almendros, A. & Gascoigne, E. Can companion animals become infected with COVID-19? *Vet. Rec.* **186**, 419-420, doi:10.1136/vr.m1322 (2020).

6 Almendros, A. Can companion animals become infected with COVID-19? *Vet. Rec.* **186**, 388-389, doi:10.1136/vr.m1194 (2020).

7 Ahmad, T. *et al.* COVID-19: Zoonotic aspects. *Travel Med. Infect. Dis.*, 101607, doi:10.1016/j.tmaid.2020.101607 (2020).

8 Ashoor, D., Ben Khalaf, N., Marzouq, M., Jarjanazi, H. & Fathallah, M. D. SARS-CoV-2 RBD mutations, ACE2 genetic polymorphism, and stability of the virus-receptor complex: The COVID-19 host-pathogen nexus. *bioRxiv*, 2020.2010.2023.352344, doi:10.1101/2020.10.23.352344 (2020).

9 Kar, S. & Leszczynski, J. From Animal to Human: Interspecies Analysis Provides a Novel Way of Ascertaining and Fighting COVID-19. *The Innovation* **1**, 100021, doi:10.1016/j.xinn.2020.100021 (2020).

10 Lan, J. *et al.* Structure of the SARS-CoV-2 spike receptor-binding domain bound to the ACE2 receptor. *Nature*, doi:10.1038/s41586-020-2180-5 (2020).

11 Abdel-Moneim, A. S. & Abdelwhab, E. M. Evidence for SARS-CoV-2 Infection of Animal Hosts. *Pathogens* **9**, 529, doi:10.3390/pathogens9070529 (2020).

12 Katsnelson, A. How do viruses leap from animals to people and spark pandemics? *98*, 26 (2020).

13 Zhang, T., Wu, Q. & Zhang, Z. Probable Pangolin Origin of SARS-CoV-2 Associated with the COVID-19 Outbreak. *Curr. Biol.* **30**, 1346-1351 e1342, doi:10.1016/j.cub.2020.03.022 (2020).

14 Luan, J., Jin, X., Lu, Y. & Zhang, L. SARS-CoV-2 spike protein favors ACE2 from Bovidae and Cricetidae. *J. Med. Virol.*, https://doi.org/10.1002/jmv.25817, doi:10.1002/jmv.25817 (2020).

15 Damas, J. *et al.* Broad host range of SARS-CoV-2 predicted by comparative and structural analysis of ACE2 in vertebrates. *Proc. Natl. Acad. Sci. U S A* **117**, 22311-22322, doi:10.1073/pnas.2010146117 (2020).

16 Luan, J., Lu, Y., Jin, X. & Zhang, L. Spike protein recognition of mammalian ACE2 predicts the host range and an optimized ACE2 for SARS-CoV-2 infection. *Biochem. Biophys. Res. Commun.*, doi:10.1016/j.bbrc.2020.03.047 (2020).

17 Gimeno, A. *et al.* Prediction of Novel Inhibitors of the Main Protease (M-pro) of SARS-CoV-2 through Consensus Docking and Drug Reposition. *Int. J. Mol. Sci.* **21**, 3793 (2020).

18 Touyz, R. M., Li, H. & Delles, C. ACE2 the Janus-faced protein - from cardiovascular protection to severe acute respiratory syndrome-coronavirus and COVID-19. *Clin. Sci.* **134**, 747-750, doi:10.1042/CS20200363 (2020).

19 Shang, J. *et al.* Structural basis of receptor recognition by SARS-CoV-2. *Nature*, doi:10.1038/s41586-020-2179-y (2020).

20 Qiu, Y. *et al.* Predicting the angiotensin converting enzyme 2 (ACE2) utilizing capability as the receptor of SARS-CoV-2. *Microbes Infect.* **22**, 221-225, doi:10.1016/j.micinf.2020.03.003 (2020).

21 Wu, C. *et al.* In Silico Analysis of Intermediate Hosts and Susceptible Animals of SARS-CoV-2. *ChemRxiv* chemrxiv.12057996.v1 (2020). doi:doi.org/10.26434/chemrxiv.12057996.v1.

22 Rodrigues, J. P. *et al.* Insights on cross-species transmission of SARS-CoV-2 from structural modeling. *bioRxiv*, 2020.2006.2005.136861, doi:10.1101/2020.06.05.136861 (2020).

23 Li, Y. *et al.* SARS-CoV-2 and three related coronaviruses utilize multiple ACE2 orthologs and are potently blocked by an improved ACE2-Ig. *J. Virol.*, doi:10.1128/JVI.01283-20 (2020).

24 Lam, S. D. *et al.* SARS-CoV-2 spike protein predicted to form complexes with host receptor protein orthologues from a broad range of mammals. *Sci Rep* **10**, 16471, doi:10.1038/s41598-020-71936-5 (2020).

25 Lam, T. T. *et al.* Identifying SARS-CoV-2-related coronaviruses in Malayan pangolins. *Nature* **583**, 282-285, doi:10.1038/s41586-020-2169-0 (2020).

26 Xiao, K. *et al.* Isolation of SARS-CoV-2-related coronavirus from Malayan pangolins. *Nature* **583**, 286-289, doi:10.1038/s41586-020-2313-x (2020).

27 Sit, T. H. C. *et al.* Infection of dogs with SARS-CoV-2. *Nature*, https://doi.org/10.1038/s41586-41020-42334-41585., doi:10.1038/s41586-020-2334-5 (2020).

28 Opriessnig, T. & Huang, Y. W. Update on possible animal sources for COVID-19 in humans. *Xenotransplantation* **27**, e12621, doi:10.1111/xen.12621 (2020).
29 Chan, J. F. *et al.* Simulation of the clinical and pathological manifestations of Coronavirus Disease 2019 (COVID-19) in golden Syrian hamster model: implications for disease pathogenesis and transmissibility. *Clin. Infect. Dis.*, doi:10.1093/cid/ciaa325 (2020).
30 Johansen, M. D. *et al.* Animal and translational models of SARS-CoV-2 infection and COVID-19. *Mucosal Immunol*, doi:10.1038/s41385-020-00340-z (2020).
31 Shi, J. *et al.* Susceptibility of ferrets, cats, dogs, and other domesticated animals to SARS-coronavirus 2. *Science* **368**, 1016-1020, doi:10.1126/science.abb7015 (2020).
32 Kim, Y. I. *et al.* Infection and Rapid Transmission of SARS-CoV-2 in Ferrets. *Cell Host Microbe* **27**, 704-709, doi:10.1016/j.chom.2020.03.023 (2020).
33 Segalés, J. *et al.* Detection of SARS-CoV-2 in a cat owned by a COVID-19−affected patient in Spain. *Proceedings of the National Academy of Sciences*, 202010817, doi:10.1073/pnas.2010817117 (2020).
34 Spinello, A., Saltalamacchia, A. & Magistrato, A. Is the Rigidity of SARS-CoV-2 Spike Receptor-Binding Motif the Hallmark for Its Enhanced Infectivity? Insights from All-Atom Simulations. *J Phys Chem Lett* **11**, 4785-4790, doi:10.1021/acs.jpclett.0c01148 (2020).
35 Wang, Y., Liu, M. & Gao, J. Enhanced receptor binding of SARS-CoV-2 through networks of hydrogen-bonding and hydrophobic interactions. . *Proc. Natl. Acad. Sci. USA* **117**, 13967-13974, doi:10.1073/pnas.2008209117 (2020).
36 Yuan, M. *et al.* A highly conserved cryptic epitope in the receptor-binding domains of SARS-CoV-2 and SARS-CoV. *Science* **368**, 630-633, doi:10.1126/science.abb7269 (2020).
37 Ge, X. Y. *et al.* Isolation and characterization of a bat SARS-like coronavirus that uses the ACE2 receptor. *Nature* **503**, 535-538, doi:10.1038/nature12711 (2013).
38 Li, W. *et al.* Angiotensin-converting enzyme 2 is a functional receptor for the SARS coronavirus. *Nature* **426**, 450-454, doi:10.1038/nature02145 (2003).
39 Wan, Y., Shang, J., Graham, R., Baric, R. S. & Li, F. Receptor Recognition by the Novel Coronavirus from Wuhan: an Analysis Based on Decade-Long Structural Studies of SARS Coronavirus. *J. Virol.* **94**, doi:10.1128/JVI.00127-20 (2020).
40 Korber, B. *et al.* Spike mutation pipeline reveals the emergence of a more transmissible form of SARS-CoV-2. *bioRxiv* 2020.04.29.069054 (2020). doi:10.1101/2020.04.29.069054.
41 Alexander, M. R. *et al.* Which animals are at risk? Predicting species susceptibility to COVID-19. *bioRxiv* 2020.07.09.194563 (2020). doi:10.1101/2020.07.09.194563.
42 Mahdy, M. A. A. An Overview of SARS-CoV-2 and Animal Infection. *Preprints* 202004.0192.v1 (2020).
43 Temmam, S. *et al.* Absence of SARS-CoV-2 infection in cats and dogs in close contact with a cluster of COVID-19 patients in a veterinary campus. *bioRxiv*2020). doi:10.1101/2020.04.07.029090.
44 Shi, J. *et al.* Susceptibility of ferrets, cats, dogs, and other domesticated animals to SARS-coronavirus 2. *Science*, doi:10.1126/science.abb7015 (2020).
45 Kim, Y. I. *et al.* Infection and Rapid Transmission of SARS-CoV-2 in Ferrets. *Cell Host Microbe*, doi:10.1016/j.chom.2020.03.023 (2020).
46 Yu, P. *et al.* Age-related rhesus macaque models of COVID-19. *Animal Model Exp Med.* , 1-5, doi:10.1002/ame2.12108 (2020).
47 Rockx, B. *et al.* Comparative pathogenesis of COVID-19, MERS And SARS in a non-human primate model. *bioRxiv* 2020.2003.2017.995639 (2020).
48 Bao, L. *et al.* The pathogenicity of 2019 novel coronavirus in hACE2 transgenic mice. *Nature* **583**, 830–833 (2020).
49 Golden, J. *et al.* Human angiotensin-converting enzyme 2 transgenic mice infected with SARS-CoV-2 develop severe and fatal respiratory disease. *bioRxiv* 2020.07.09.195230 (2020). doi:10.1101/2020.07.09.195230.
50 Huang, J., Song, W., Huang, H. & Sun, Q. Pharmacological therapeutics targeting RNA-dependent RNA polymerase, proteinase and spike protein: from mechanistic studies to clinical trials for COVID-19. *J. Clin. Med.* **9**, 1131 (2020).
51 Temmam, S. *et al.* Absence of SARS-CoV-2 infection in cats and dogs in close contact with a cluster of COVID-19 patients in a veterinary campus. *bioRxiv* 2020.04.07.029090 (2020). doi:10.1101/2020.04.07.029090.
52 Goumenou, M., Spandidos, D. A. & Tsatsakis, A. [Editorial] Possibility of transmission through dogs being a contributing factor to the extreme Covid19 outbreak in North Italy. *Mol Med Rep* **21**, 2293-2295, doi:10.3892/mmr.2020.11037 (2020).
53 Wrobel, A. G. *et al.* SARS-CoV-2 and bat RaTG13 spike glycoprotein structures inform on virus evolution and furin-cleavage effects. *Nat. Struct. Mol. Biol.*, https://doi.org/10.1038/s41594-41020-40468-41597, doi:10.1038/s41594-020-0468-7 (2020).

54 Casadevall, A. & Imperiale, M. J. Risks and benefits of gain-of-function experiments with pathogens of pandemic potential, such as influenza virus: a call for a science-based discussion. *mBio* **5**, e01730-01714, doi:10.1128/mBio.01730-14 (2014).
55 Day, T., Gandon, S., Lion, S. & Otto, S. P. On the evolutionary epidemiology of SARS-CoV-2. *Curr. Biol.*, doi:https://doi.org/10.1016/j.cub.2020.06.031 (2020).
56 Rambaut, A. in *Virological.org* (2020).
57 Pettersen, E. F. *et al.* UCSF Chimera--a visualization system for exploratory research and analysis. *J. Comput. Chem.* **25**, 1605-1612, doi:10.1002/jcc.20084 (2004).
58 Sali, A. & Blundell, T. L. Comparative protein modelling by satisfaction of spatial restraints. *J. Mol. Biol.* **234**, 779-815, doi:10.1006/jmbi.1993.1626 (1993).
59 John, B. & Sali, A. Comparative protein structure modeling by iterative alignment, model building and model assessment. *Nucleic Acids Res.* **31**, 3982-3992, doi:10.1093/nar/gkg460 (2003).
60 Shen, M. Y. & Sali, A. Statistical potential for assessment and prediction of protein structures. *Protein Sci.* **15**, 2507-2524, doi:10.1110/ps.062416606 (2006).
61 Benkert, P., Biasini, M. & Schwede, T. Toward the estimation of the absolute quality of individual protein structure models. *Bioinform.* **27**, 343-350, doi:10.1093/bioinformatics/btq662 (2011).
62 Chen, V. B. *et al.* MolProbity: all-atom structure validation for macromolecular crystallography. *Acta Crystallogr D Biol Crystallogr* **66**, 12-21, doi:10.1107/S0907444909042073 (2010).
63 Walls, A. C. *et al.* Structure, Function, and Antigenicity of the SARS-CoV-2 Spike Glycoprotein. *Cell* **181**, 281-292, doi:10.1016/j.cell.2020.02.058 (2020).
64 Yan, Y., Zhang, D., Zhou, P., Li, B. & Huang, S. Y. HDOCK: a web server for protein-protein and protein-DNA/RNA docking based on a hybrid strategy. *Nucleic Acids Res* **45**, W365-W373, doi:10.1093/nar/gkx407 (2017).
65 Yan, Y., Tao, H., He, J. & Huang, S. Y. The HDOCK server for integrated protein-protein docking. *Nat Protoc*, doi:10.1038/s41596-020-0312-x (2020).
66 Abraham, M. J. *et al.* GROMACS; High performance molecular simulations through multi-level parallelism from laptops to supercomputers. *SoftwareX* **1-2**, 19-25 (2015).
67 Baker, N. A., Sept, D., Joseph, S., Holst, M. J. & McCammon, J. A. Electrostatics of nanosystems: application to microtubules and the ribosome. *Proc. Natl. Acad. Sci. U S A* **98**, 10037-10041, doi:10.1073/pnas.181342398 (2001).
68 Kumari, R., Kumar, R., Open Source Drug Discovery, C. & Lynn, A. g_mmpbsa--a GROMACS tool for high-throughput MM-PBSA calculations. *J. Chem. Inf. Model.* **54**, 1951-1962, doi:10.1021/ci500020m (2014).
69 Wang, E. *et al.* End-Point Binding Free Energy Calculation with MM/PBSA and MM/GBSA: Strategies and Applications in Drug Design. *Chem Rev* **119**, 9478-9508, doi:10.1021/acs.chemrev.9b00055 (2019).

In silico comparison of SARS-CoV-2 spike protein-ACE2 binding affinities across species and implications for viral origin

Sakshi Piplani[1,2], Puneet Kumar Singh[2], David A. Winkler[3-6]*, Nikolai Petrovsky[1,2]*

[1] College of Medicine and Public Health, Flinders University, Bedford Park 5046, Australia

[2] Vaxine Pty Ltd, 11 Walkley Avenue, Warradale 5046, Australia

[3] La Trobe University, Kingsbury Drive, Bundoora 3086, Australia

[4] Monash Institute of Pharmaceutical Sciences, Monash University, Parkville 3052, Australia

[5] School of Pharmacy, University of Nottingham, Nottingham NG7 2RD. UK

[6] CSIRO Data61, Pullenvale 4069, Australia

SUPPLEMENTARY INFORMATION

Supplementary Table 1. Human template structures used to model selected ACE2 species and similarity scores of each ACE2 sequence to the selected template used.

Species	Accession No.	Database	Template	Similarity
Rhinolophus sinicus (Bat)	AGZ48803.1	UniProt	3SCI	79.73%
Mus musculus (Mouse)	Q8R0I0	UniProt	1R42	84.27%
Mustela putorius furo (Ferret)	Q2WG88	UniProt	1R42	83.44%
Mesocricetus auratus (Hamster)	A0A1U7QTA1	UniProt	1R42	87.58%
Felis catus (Cat)	Q56H28	UniProt	1R42	85.93%
Canis luparis (Dog)	J9P7Y2	UniProt	1R42	84.93%
Paguma larvata (Ccivet)	Q56NL1	UniProt	3D0G†	86.77%
Macaca fascicularis (Monkey)	A0A2K5X283	UniProt	1R42	96.91%
Manis javanica (Pangolin)	XP_017505752.1	NCBI	1R42	85.57%
Ophiophagus hannah (King cobra)	V8NIH2	UniProt	1R42	61.42%
Equus caballus (Horse)	F6V9L3	UniProt	6MI7	85.91%
Panthera tigris altaica (Tiger)	XP_007090142.1	NCBI	6MI7	85.91%
Bos taurus (Cow)	NP_001019673.2	NCBI	6MI7	80.30%

† ACE2 structure from spike protein receptor-binding domain from the 2002-2003 SARS coronavirus human strain complexed with human-civet chimeric receptor ACE2

Supplementary Table 2. MolProbity and Ramachandran scores for ACE2 modelled structures for selected species

Species	**MolProbity Score**	**Ramachandran Score (favoured region)**
Rhinolophus sinicus (bat)	2.45	97.8%
Mus musculus (mouse)	2.49	98.2%
Mustela putorius furo (ferret)	2.5	98.3%
Mesocricetus auratus (hamster)	2.59	98.7%
Felis catus (cat)	2.42	98.5%
Paguma larvata (civet)	2.52	97.3%
Macaca fascicularis (monkey)	2.59	98.2%
Manis javanica (pangolin)	2.42	98.3%
Ophiophagus hannah (king cobra)	2.93	96.0%
Canis lupus familiaris (dog)	2.9	97.1%
Equus caballus (horse)	2.29	96.3%
Panthera tigris altaica (tiger)	2.25	96.6%
Bos Taurus (cattle)	2.70	96.2%

Supplementary Table 3. RMSD for alignments of Cα backbones for ACE2, and the whole ACE2spike complex generated by homology modelling (Modeller) and HDOCK.

Species	RMSD Å Cα ACE2	RMSD Å complex
Bat	0.82	0.88
Cat	0.54	0.85
Cattle	0.77	0.79
Civet	0.74	0.85
Dog	0.69	0.82
Ferret	0.59	0.84
Hamster	0.60	0.85
Horse	0.82	0.84
Monkey	0.56	0.85
Pangolin	0.54	0.86
Snake	0.84	0.89
Tiger	0.87	0.85
Mouse	0.54	0.86

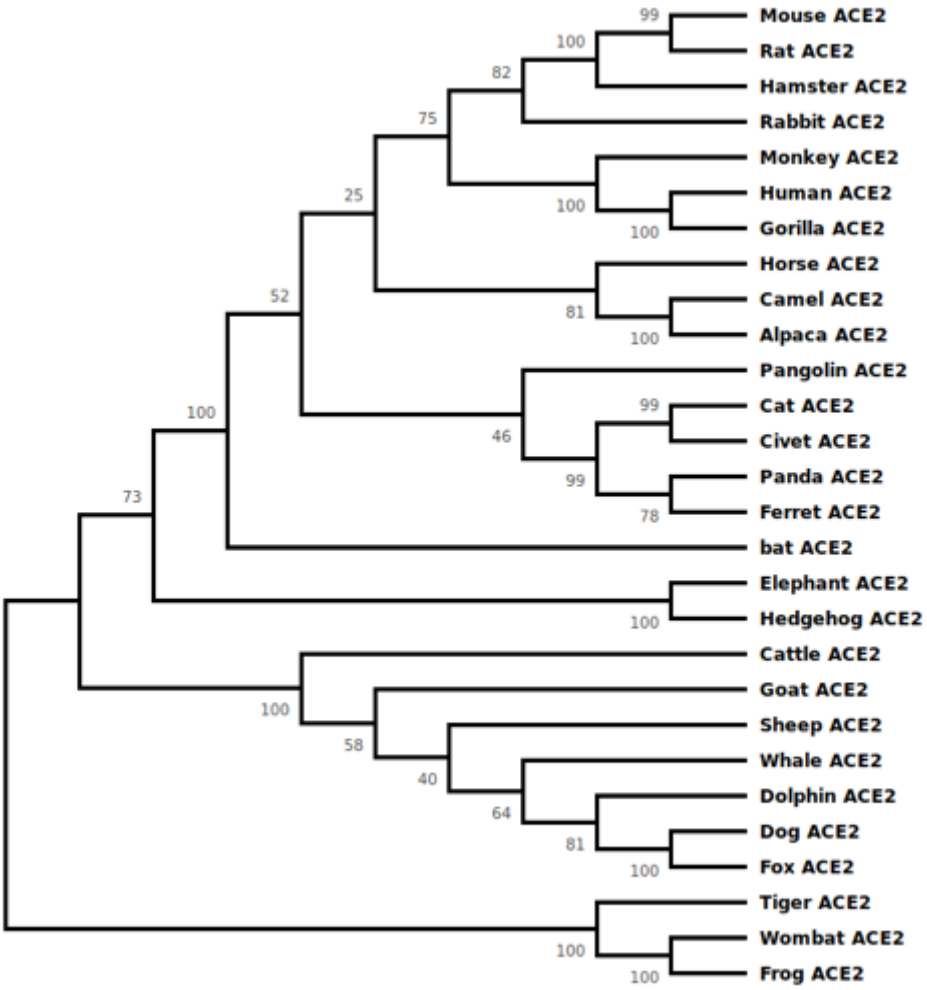

Supplementary Figure 1. Phylogenetic tree showing relatedness of sequences of ACE2 proteins from selected species.

```
Ophiophagus     MLMKQAPVRKPSSRSFTHPAFFDLKGNMLTWLCLTWSLVVLALAQ-DETKVATKFLEQFD  59
Mesocricetus    ------------------------MSSSSWLLLS--LVAVTTAQSIIEEQAKTFLDKFN  33
Mus             ------------------------MSSSSWLLLS--LVAVTTAQSLTEENAKTFLNNFN  33
Rhinolophus     ------------------------MSGSSWLLLS--LVAVTTAQSTTEDEAKMFLDKFN  33
Bos             ------------------------MTGSFWLLLS--LVAVTAAQSTTEEQAKTFLEKFN  33
Homo            ------------------------MSSSSWLLLS--LVAVTAAQSTIEEQAKTFLDKFN  33
Macaca          ------------------------MSGSSWLLLS--LVAVTAAQSTIEEQAKTFLDKFN  33
Mustela         ------------------------MLGSSWLLLS--LAALTAAQSTTEDLAKTFLEKFN  33
Canis           ------------------------MSGSSWLLLS--LAALTAAQS-TEDLVKTFLEKFN  32
Paguma          ------------------------MSGSFWLLLS--FAALTAAQSTTEELAKTFLETFN  33
Felis           ------------------------MSGSFWLLLS--FAALTAAQSTTEELAKTFLEKFN  33
Panthera        ---------------------------------LS--FAALTAAQSTTEELAKTFLEKFN  25
Manis           ------------------------MSGSSWLLLS--LVAVTAAQSTSDEEAKTFLEKFN  33
Equus           ------------------------MSGSSWLLLS--LVAVTAAQSTTEDLAKTFLEKFN  33
                                                  *:  :..:: **    . .. **: *:

Ophiophagus     ARATDLYYNASIASWNYNTNLTEENAKIMHEKDNIFSKFYGEACRNASMFNVNHITDETI  119
Mesocricetus    QEAEDLSYQSALASWNYNTNITEENAQKMNEAAAKWSAFYEEQSKLAKNYSLQEVQNLTI  93
Mus             QEAEDLSYQSSLASWNYNTNITEENAQKMSEAAAKWSAFYEEQSKTAQSFSLQEIQTPII  93
Rhinolophus     TKAEDLSHQSSLASWDYNTNINDENVQKMDEAGAKWSAFYEEQSKLAKNYSLEQIQNVTV  93
Bos             HEAEDLSYQSSLASWNYNTNITDENVQKMNEARAKWSAFYEEQSRMAKTYSLEEIQNLTL  93
Homo            HEAEDLFYQSSLASWNYNTNITEENVQNMNNAGDKWSAFLKEQSTLAQMYPLQEIQNLTV  93
Macaca          HEAEDLFYQSSLASWNYNTNITEENVQNMNNAGEKWSAFLKEQSTLAQMYPLQEIQNLTV  93
Mustela         YEAEELSYQNSLASWNYNTNITDENIQKMNIAGAKWSAFYEEESQHAKTYPLEEIQDPII  93
Canis           YEAEELSYQSSLASWNYNITDENVQKMNNAGAKWSAFYEEQSKLAKTYPLEEIQDSTV  92
Paguma          YEAQELSYQSSVASWNYNTNITDENAKNMNEAGAKWSAYYEEQSKLAQTYPLAEIQDAKI  93
Felis           HEAEELSYQSSLASWNYNTNITDENVQKMNEAGAKWSAFYEEQSKLAKTYPLAEIHNTTV  93
Panthera        HEAEELSYQSSLASWNYNTNITDENVQKMNEAGAKWSAFYEEQSKLAETYPLAEIHNTTV  85
Manis           SEAEELSYQSSLASWNYNTNITDENVQKMNVAGAKWSTFYEEQSKIAKNYQLQNIQNDTI  93
Equus           SEAEELSHQSSLASWSYNTNITDENVQKMNEAGARWSAFYEEQCKLAKTYPLEEIQNLTV  93
                 .* :* :: ::***.** *:.:** : *      :* :  * .  *. : : .:    :

Ophiophagus     KLQIRLLQSGSTD----STKDQLDTVLHKMSTLYS-------------------LDDIMA  156
Mesocricetus    KRQLQALQQSGSSALSADKNKQLNTILNTMSTIYSTGKVCNPKNPQECLLLEPGLDDIMA  153
Mus             KRQLQALQQSGSSALSADKNKQLNTILNTMSTIYSTGKVCNPKNPQECLLLEPGLDEIMA  153
Rhinolophus     KLQLQILQQSGSPVLSEDKSKRLNSILNAMSTIYSTGKVCKPNKPQECLLLEPGLDNIMG  153
Bos             KRQLKALQHSGTSALSAEKSKRLNTILNKMSTIYSTGKVLDPN-TQECLALEPGLDDIME  152
Homo            KLQLQALQQNGSSVLSEDKSKRLNTILNTMSTIYSTGKVCNPDNPQECLLLEPGLNEIMA  153
Macaca          KLQLQALQQNGSSVLSEDKSKRLNTILNTMSTIYSTGKVCNPNNPQECLLLDPGLNEIME  153
Mustela         KRQLRALQQSGSSVLSADKRERLNTILNAMSTIYSTGKACNPNNPQECLLLEPGLDDIME  153
Canis           KRQLRALQHSGSSVLSADKNQRLNTILNSMSTIYSTGKACNPSNPQECLLLEPGLDDIME  152
Paguma          KRQLQALQQSGSSVLSADKSQRLNTILNAMSTIYSTGKACNPNNPQECLLLEPGLDNIME  153
Felis           KRQLQALQQSGSSVLSADKSQRLNTILNAMSTIYSTGKACNPNNPQECLLLEPGLDDIME  153
Panthera        KRQLQALQQSGSSVLSADKSQRLNTILNAMSTIYSTGKACNPNNPQECLLLEPGLDDIME  145
Manis           KRQLQALQLSGSSALSADKNQRLNTILNTMSTIYSTGKVCNPGNPQECSLLEPGLDNIME  153
Equus           KRQLQALQQSGSSVLSADKSKRLNEILNTMSTIYSTGKVCNPSNPQECLLLEPGLDAIME  153
                * *:: ** ..:     .. .:*: :*: ***:**                    *: **

Ophiophagus     NNWNYPERLWAWEGWRANVGKKMRPLYETYVELKNKYARLRGYADYGDYWRANYEVDLPG  216
Mesocricetus    TSTDYNERLWAWEGWRAEVGKQLRPLYEEYVVLKNEMARANNYEDYGDYWRGDYEAEGAD  213
Mus             TSTDYNSRLWAWEGWRAEVGKQLRPLYEEYVVLKNEMARANNYNDYGDYWRGDYEAEGAD  213
Rhinolophus     TSKDYNERLWAWEGWRAEVGKQLRPLYEEYVVLKNEMARGYHYEDYGDYWRRDYETEESP  213
Bos             NSRDYNRRLWAWEGWRAEVGKQLRPLYEEYVVLENEMARANNYEDYGDYWRGDYEVTGAG  212
Homo            NSLDYNERLWAWESWRSEVGKQLRPLYEEYVVLKNEMARANHYEDYGDYWRGDYEVNGVD  213
Macaca          KSLDYNERLWAWEGWRSEVGKQLRPLYEEYVVLKNEMARANHYKDYGDYWRGNYEVNGVD  213
Mustela         NSKDYNERLWAWEGWRSEVGKQLRPLYEEYVALKNEMARANNYEDYGDYWRGDYEEEWAD  213
Canis           NSKDYNERLWAWEGWRSEVGKQLRPLYEEYVALKNEMARANNYEDYGDYWRGDYEEEWEN  212
Paguma          NSKDYNERLWAWEGWRAEVGKQLRPLYEEYVALKNEMARANNYEDYGDYWRGDYEEEWTG  213
Felis           NSKDYNERLWAWEGWRAEVGKQLRPLYEEYVALKNEMARANNYEDYGDYWRGDYEEEWTD  213
Panthera        NSKDYNERLWAWEGWRAEVGKQLRPLYEEYVALKNEMARANNYEDYGDYWRGDYEEEWTD  205
Manis           SSKDYNERLWAWEGWRSEVGKQLRPLYEEYVVLKNEMARANHYEDYGDYWRGDYEAEGAN  213
Equus           NSKDYNQRLWAWEGWRSEVGKQLRPLYEEYVVLKNEMARANNYEDYGDYWRGDYEAEGPS  213
                .. :*  ******.**::***::***** ** *:*: **    * ******* :**

Ophiophagus     KFQYQREQLITDVESTFKQ------QLHAYVRHHLYKRYGPELINPEGAIPAHLLGDMWG  270
Mesocricetus    GYNYNGNQLIEDVERTFKEIKPLYEQLHAYVRTKLMNTY-PSYISPTGCLPAHLLGDMWG  272
Mus             GYNYNRNQLIEDVERTFAEIKPLYEHLHAYVRRKLMDTY-PSYISPTGCLPAHLLGDMWG  272
Rhinolophus     GPGYSRDQLMKDVERIFTEIKPLYEHLHAYVRAKLMDTY-PFHISPTGCLPAHLLGDMWG  272
Bos             DYDYSRDQLMKDVERTFAEIKPLYEQLHAYVRAKLMHTY-PSYISPTGCLPAHLLGDMWG  271
Homo            GYDYSRGQLIEDVEHTFEEIKPLYEHLHAYVRAKLMNAY-PSYISPIGCLPAHLLGDMWG  272
Macaca          GYDYNRDQLIEDVERTFEEIKPLYEHLHAYVRAKLMNAY-PSYISPTGCLPAHLLGDMWG  272
Mustela         GYSYSRNQLIEDVEHTFTQIKPLYEHLHAYVRAKLMDAY-PSRISPTGCLPAHLLGDMWG  272
Canis           GYNYSRNQLIDDVEHTFTQIMPLYQHLHAYVRTKLMDTY-PSYISPTGCLPAHLLGDMWG  271
Paguma          GYNYSRNQLIQDVEDTFEQIKPLYQHLHAYVRAKLMDTY-PSRISRTGCLPAHLLGDMWG  272
Felis           GYNYSRSQLIKDVEHTFTQIKPLYQHLHAYVRAKLMDTY-PSRISPTGCLPAHLLGDMWG  272
Panthera        GYNYSRSQLIKDVEHTFTQIKPLYQHLHAYVRAKLMDSY-PSRISPTGCLPAHLLGDMWG  264
Manis           GYNYSRDHLIEDVEHIFTQIKPLYEHLHAYVRAKLMDNY-PSHISPTGCLPAHLLGDMWG  272
Equus           GYDYSRDQLIEDVERTFAEIKPLYEHLHAYVRAKLMDTY-PSHINPTGCLPAHLLGDMWG  272
                   *.  :*: ***  * :      :****** :* . * *  *.  *.:**********

Ophiophagus     RFWTNLYPLMVPYPNKTSIDVTSAMEKKKWTVNSIFKAAEHFFISIGLFNMTVGFWKNSM  330
Mesocricetus    RFWTNLYPLTVPFGQKPNIDVTDAMVNQGWNAERIFKEAEKFFVSVGLPYMTQGFWENSM  332
Mus             RFWTNLYPLTVPFAQKPNIDVTDAMMNQGWDAERIFQEAEKFFVSVGLPHMTQGFWANSM  332
Rhinolophus     RFWTNLYPLTVPFGQKPNIDVTDEMLKQGWDADRIFKEAEKFFVSVGLPNMTEGFWNNSM  332
Bos             RFWTNLYSLTVPFEHKPSIDVTEKMENQSWDAERIFKEAEKFFVSISLPYMTQGFWDNSM  331
Homo            RFWTNLYSLTVPFGQKPNIDVTDAMVDQAWDAQRIFKEAEKFFVSVGLPNMTQGFWENSM  332
Macaca          RFWTNLYSLTVPFGQKPNIDVTDAMVNQAWNAQRIFKEAEKFFVSVGLPNMTQGFWENSM  332
Mustela         RFWTNLYPLMVPFRQKPNIDVTDAMVNQSWDARRIFEEAETFFVSVGLPNMTEGFWQNSM  332
Canis           RFWTNLYPLTVPFGQKPNIDVTNAMVNQSWDARKIFKEAEKFFVSVGLPNMTQEFWENSM  331
Paguma          RFWTNLYPLTVPFGQKPNIDVTDAMVNQNWDARRIFKEAEKFFVSVGLPNMTQGFWENSM  332
Felis           RFWTNLYPLTVPFGQKPNIDVTDAMVNQSWDARRIFKEAEKFFVSVGLPNMTQGFWENSM  332
Panthera        RFWTNLYPLTVPFGQKPNIDVTDAMVNQSWDARRIFKEAEKFFVSVGLPNMTQGFWENSM  324
Manis           RFWTNLYPLTVPFRQKPNIDVTDAMVNQTWDANRIFKEAEKFFVSVGLPKMTQTFWENSM  332
Equus           RFWTNLYSLTVPFGQKPNIDVTDAMVDQSWDAKRIFEEAEKFFVSVGLPNMTQGFWENSM  332
                ******* * **: :* .****. * .: * .  **: ** **:*:.*  **  ** ***

Ophiophagus     LEEPKGGRKVVCHPTAWDMGKEDYRIKMCTKINMEDFLTAHHEMGHIEYDMAYANQPFLL  390
Mesocricetus    LTDPGDDRKVVCHPTAWDLGKGDFRIKMCTKVTMDNFLTAHHEMGHIQYDMAYATQPFLL  392
Mus             LTEPADGRKVVCHPTAWDLGHGDFRIKMCTKVTMDNFLTAHHEMGHIQYDMAYARQPFLL  392
Rhinolophus     LTEPGDGRKVVCHPTAWDLGKGDFRIKMCTKVTMEDFLTAHHEMGHIQYDMAYASQPYLL  392
Bos             LTEPGDGRKVVCHPTAWDLGKGDFRIKMCTKVTMDDFLTAHHEMGHIQYDMAYAAQPYLL  391
Homo            LTDPGNVQKAVCHPTAWDLGKGDFRILMCTKVTMDDFLTAHHEMGHIQYDMAYAAQPFLL  392
Macaca          LTDPGNVQKVVCHPTAWDLGKGDFRIIMCTKVTMDDFLTAHHEMGHIQYDMAYAAQPFLL  392
Mustela         LTEPGDNRKVVCHPTAWDLGKRDFRIKMCTKVTMDDFLTAHHEMGHIQYDMAYAEQPFLL  392
Canis           LTEPSDSRKVVCHPTAWDLGKGDFRIKMCTKVTMDDFLTAHHEMGHIQYDMAYAAQPFLL  391
Paguma          LTEPGDGRKVVCHPTAWDLGKGDFRIKMCTKVTMDDFLTAHHEMGHIQYDMAYAAQPFLL  392
Felis           LTEPGDSRKVVCHPTAWDLGKGDFRIKMCTKVTMDDFLTAHHEMGHIQYDMAYAVQPFLL  392
Panthera        LTEPGNSQKVVCHPTAWDLGKGDFRIKMCTKVTMDDFLTAHHEMGHIQYDMAYAVQPFLL  384
Manis           LTEPGDGRKVVCHPTAWDLGKHDFRIKMCTKVTMDDFLTAHHEMGHIQYDMAYAMQPYLL  392
Equus           LTEPGDGRKVVCHPTAWDLGKGDFRIKMCTKVTMDDFLTAHHEMGHIQYDMAYAVQPYLL  392
                * :* . :*.********:*: *:** ****:.*::***********:****** **:**
```

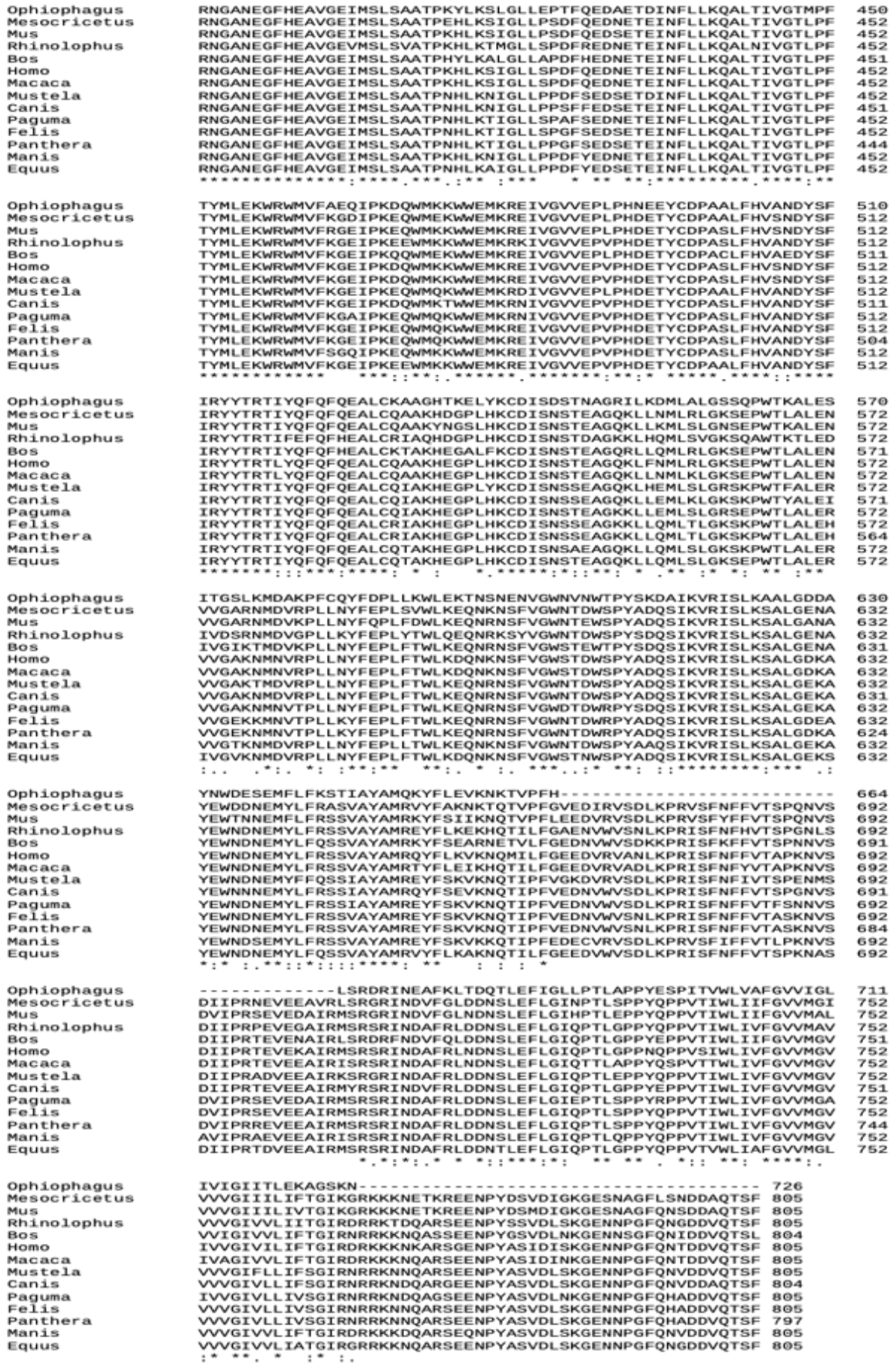

Supplementary Figure 2. Sequence alignment of ACE2 amino acid sequence from selected species. The SAR-Cov-2 spike protein binding region is highlighted in red.

BAT ACE2

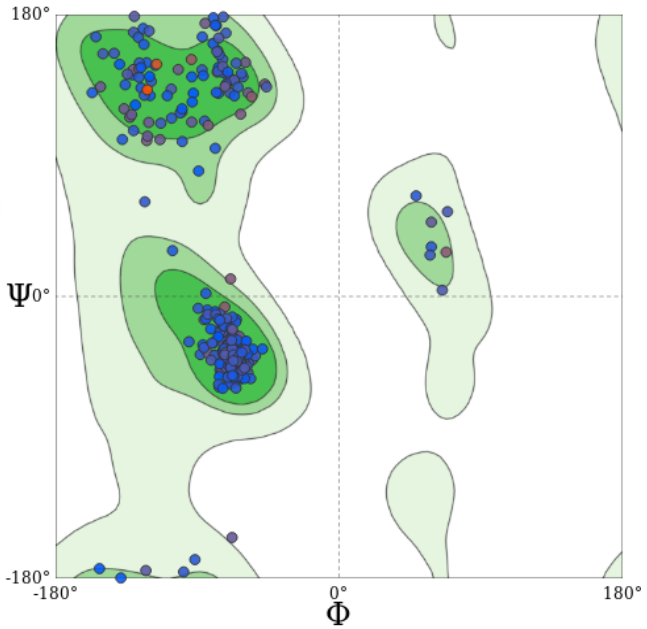

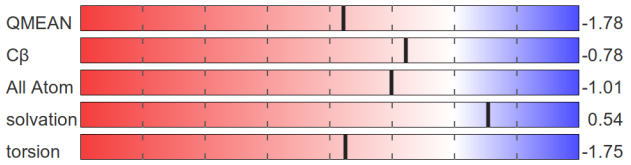

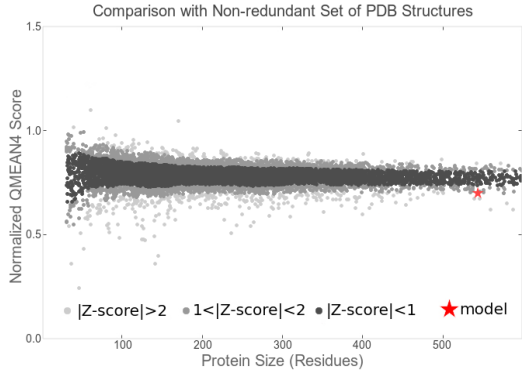

CAT ACE2

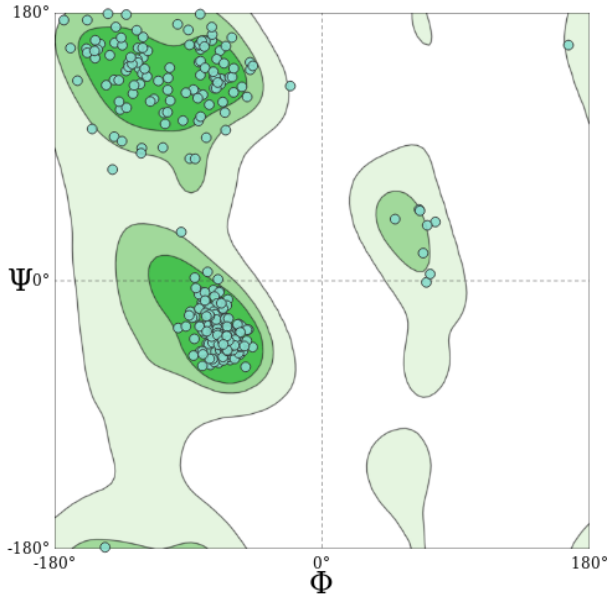

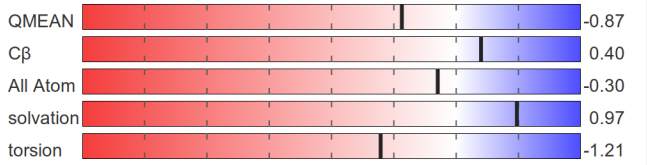

CIVET ACE2

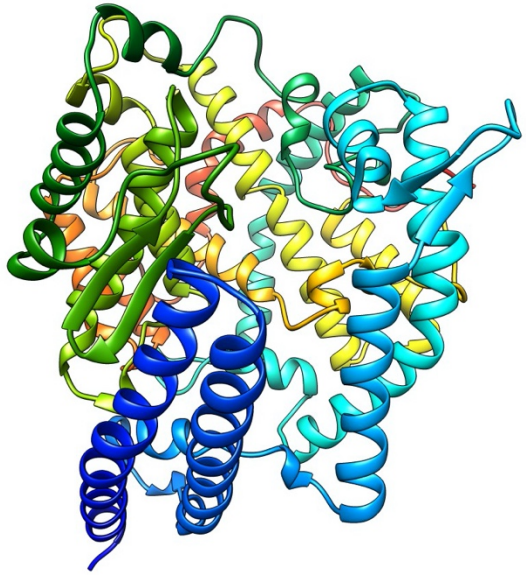

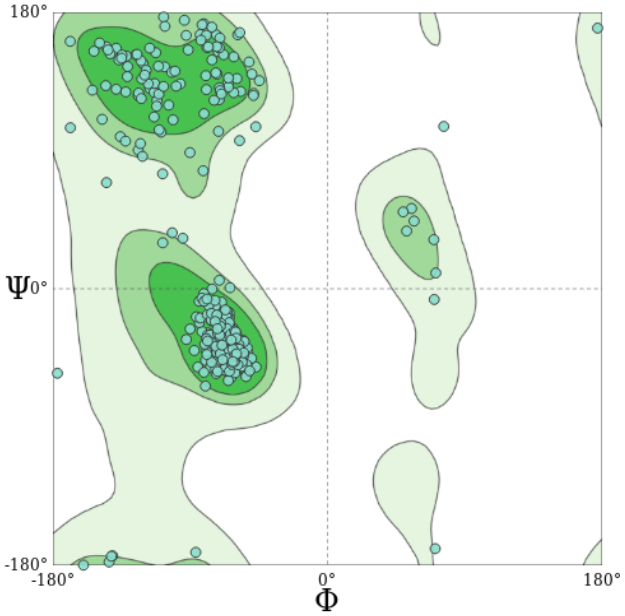

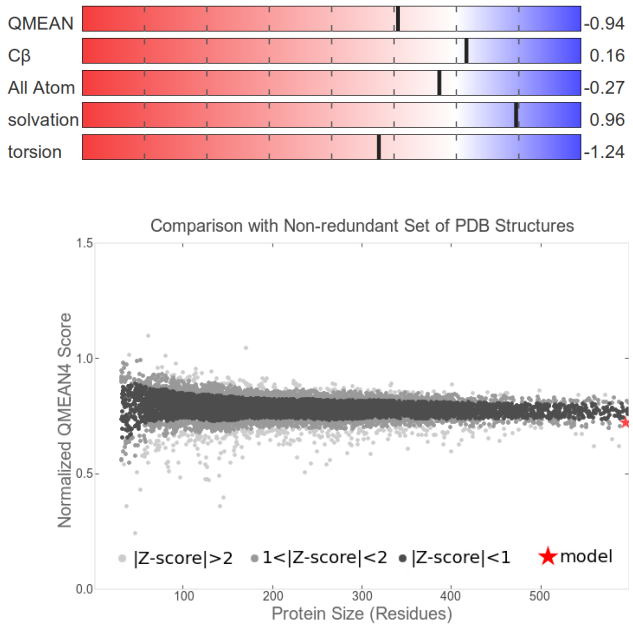

DOG ACE2

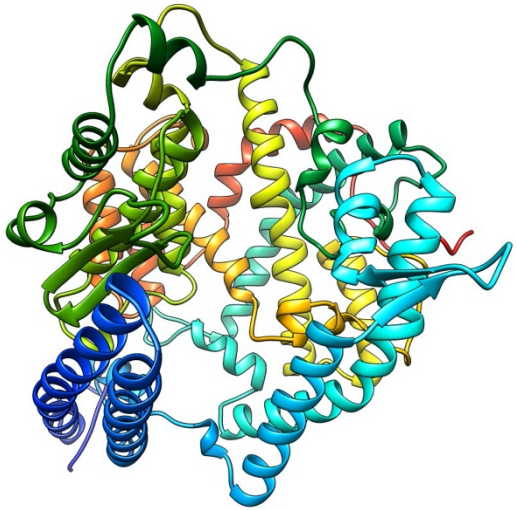

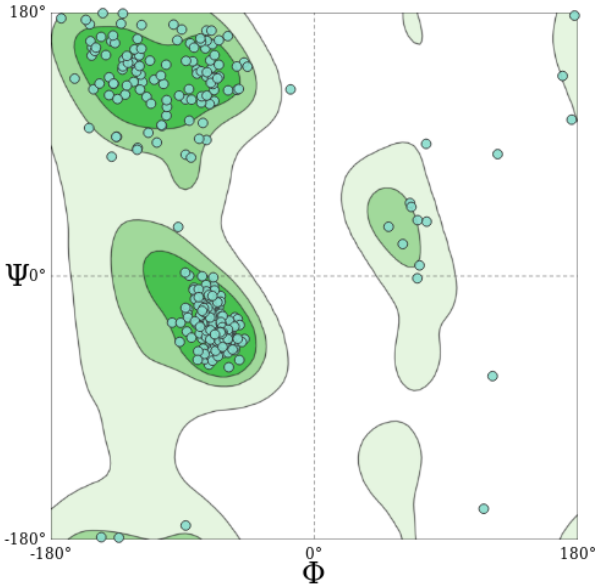

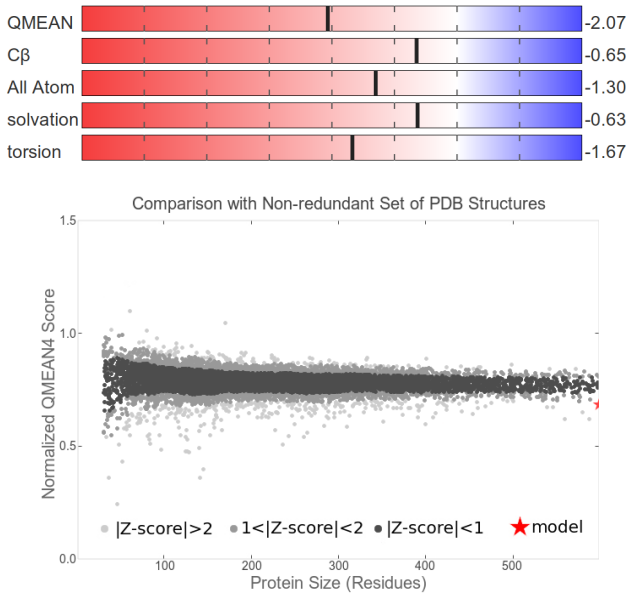

FERRET ACE2

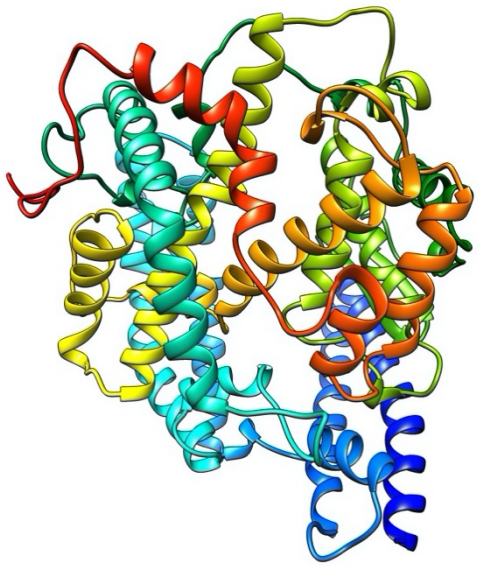

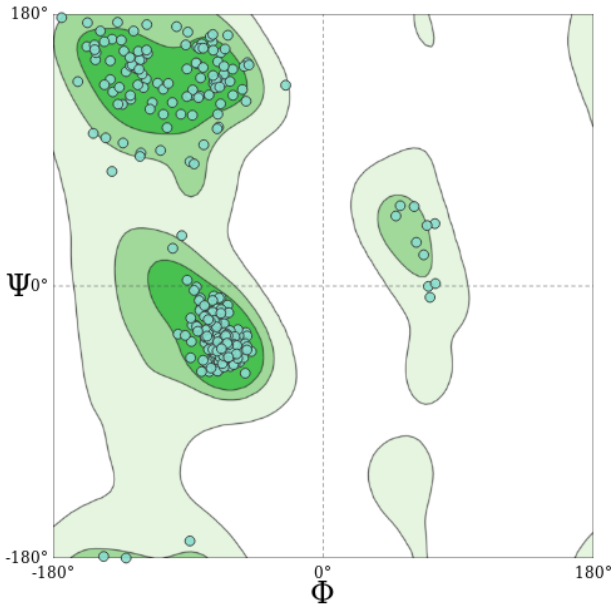

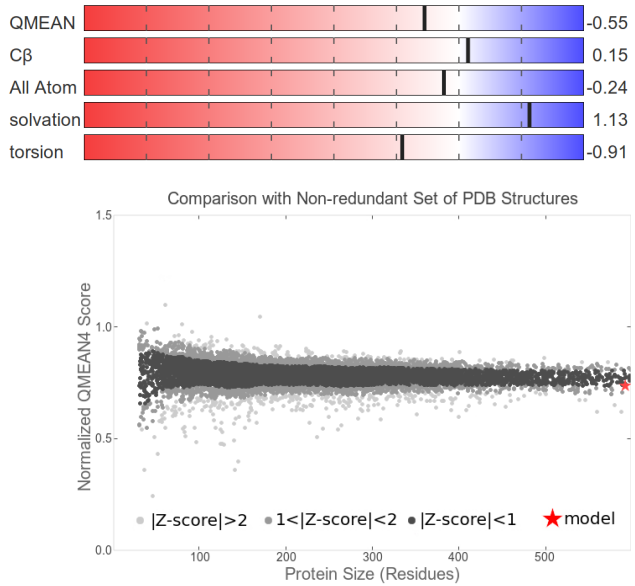

HAMSTER ACE2

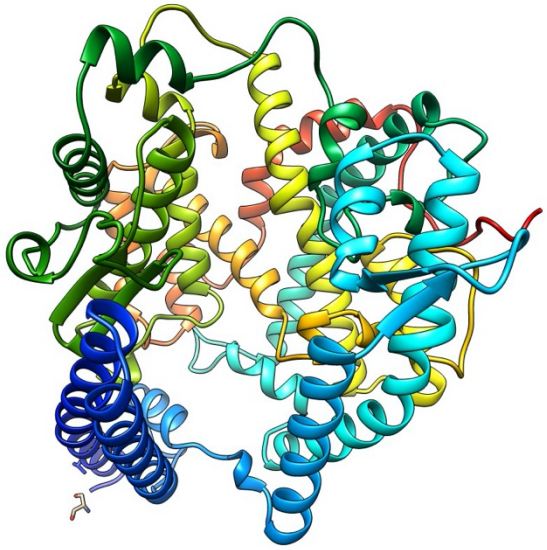

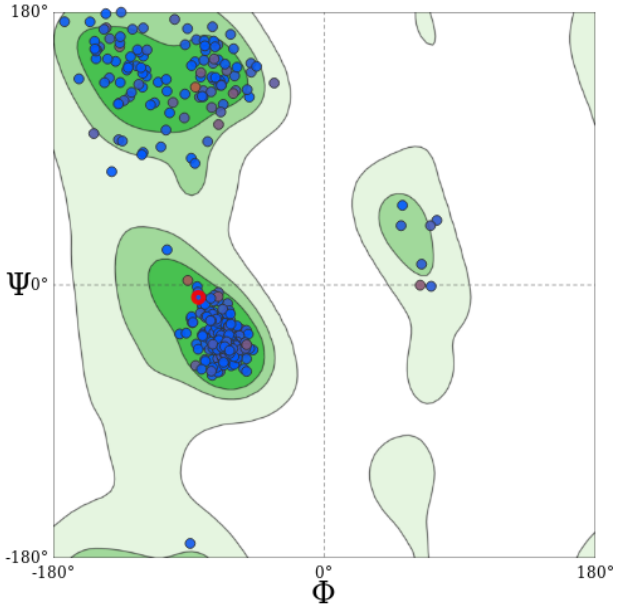

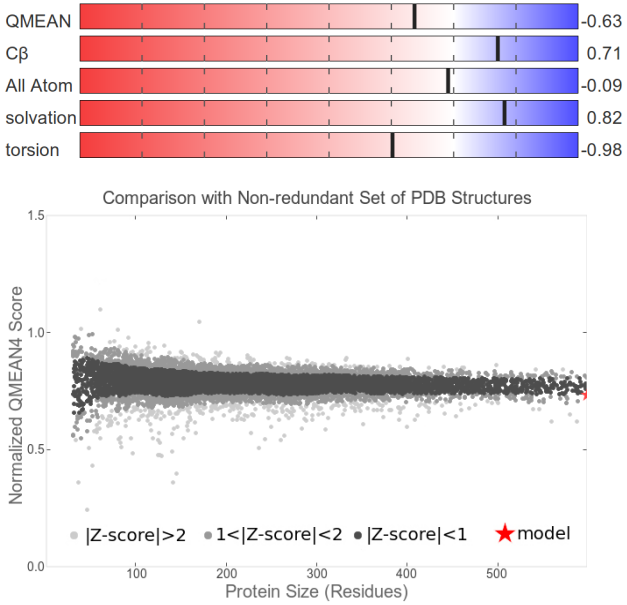

MONKEY ACE2

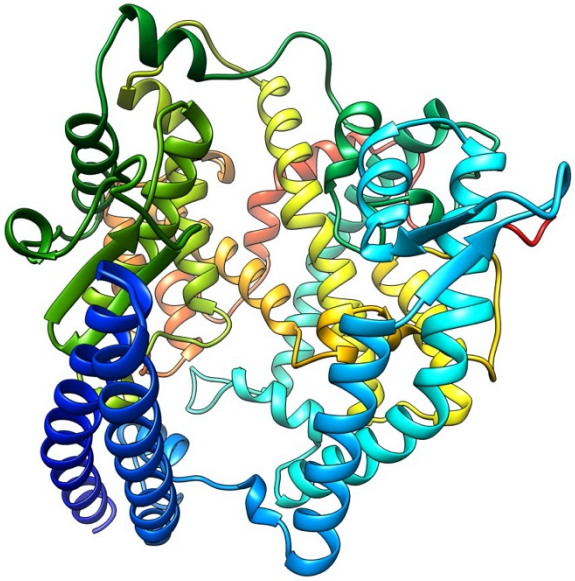

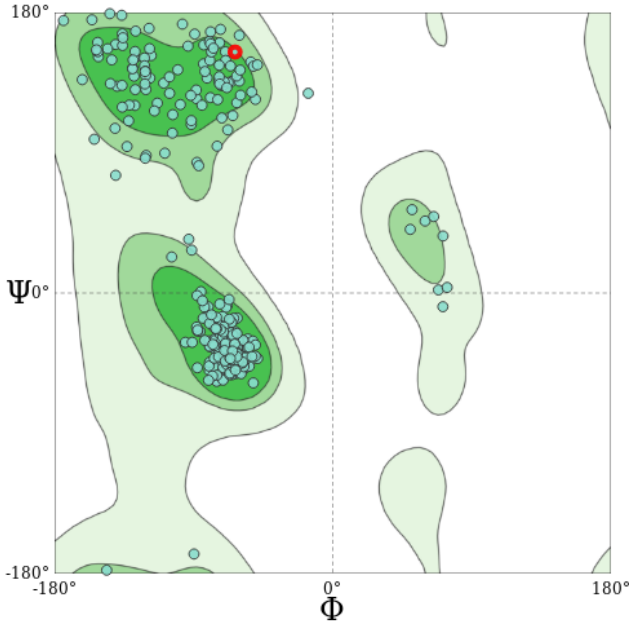

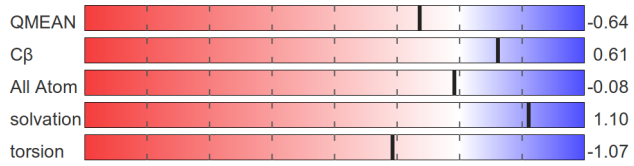

MOUSE ACE2

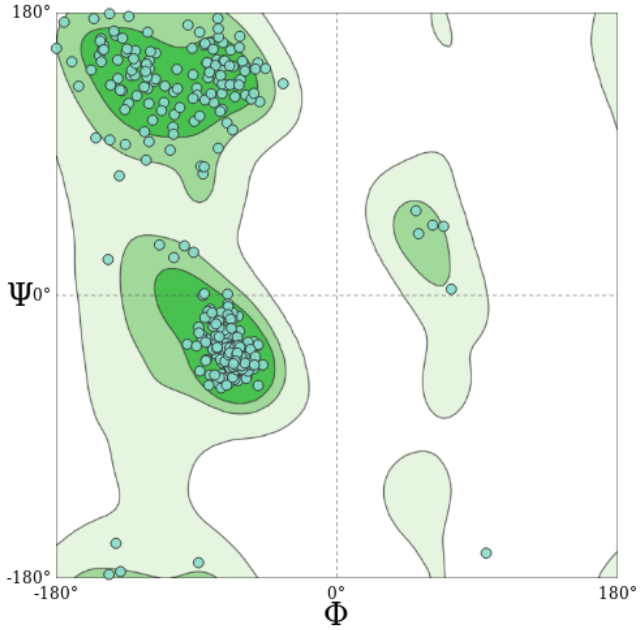

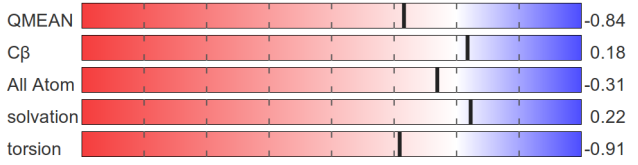

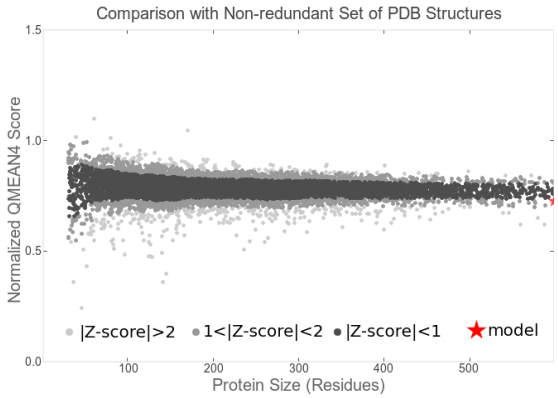

PANGOLIN ACE2

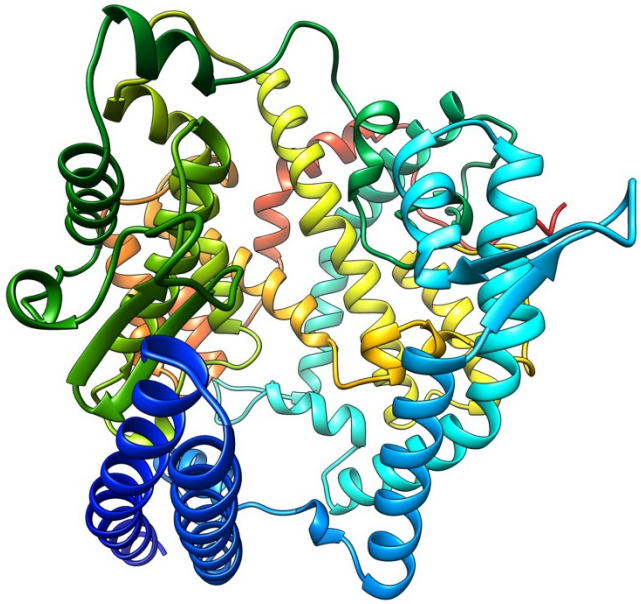

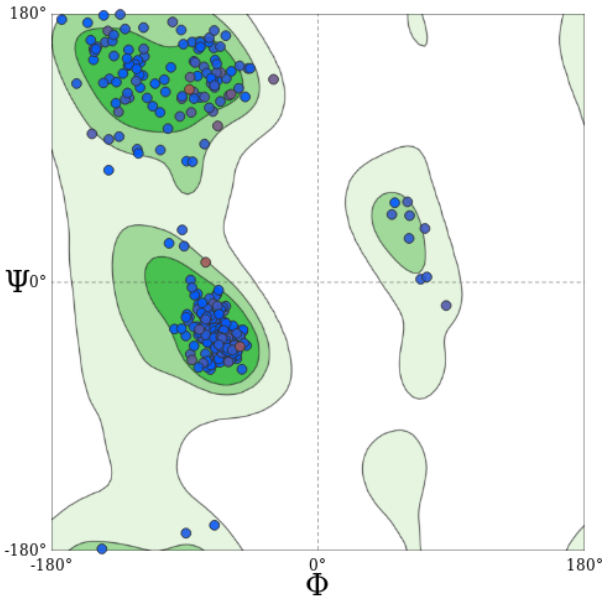

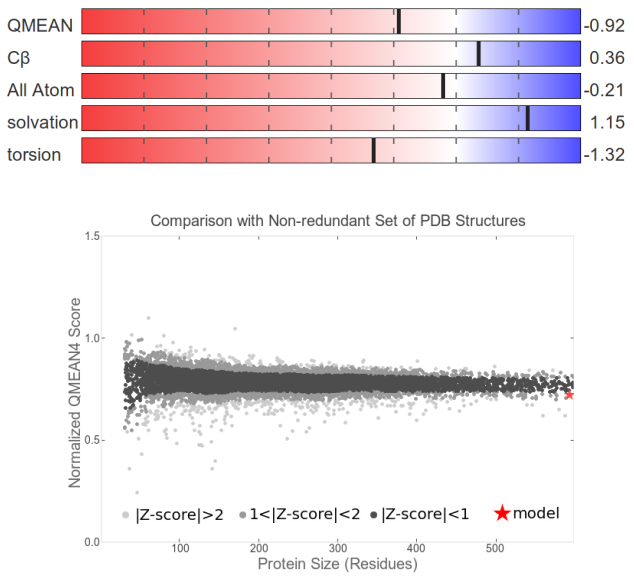

SNAKE ACE2

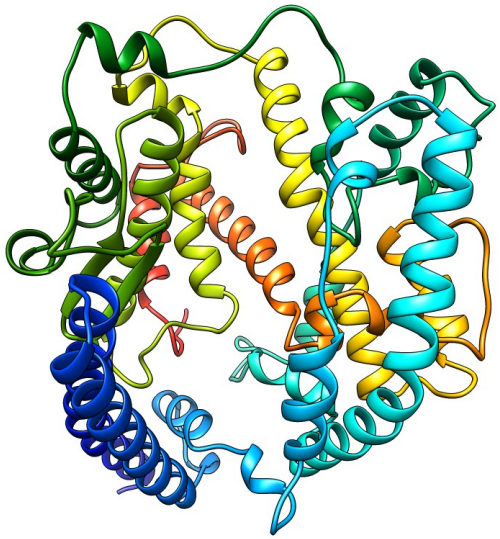

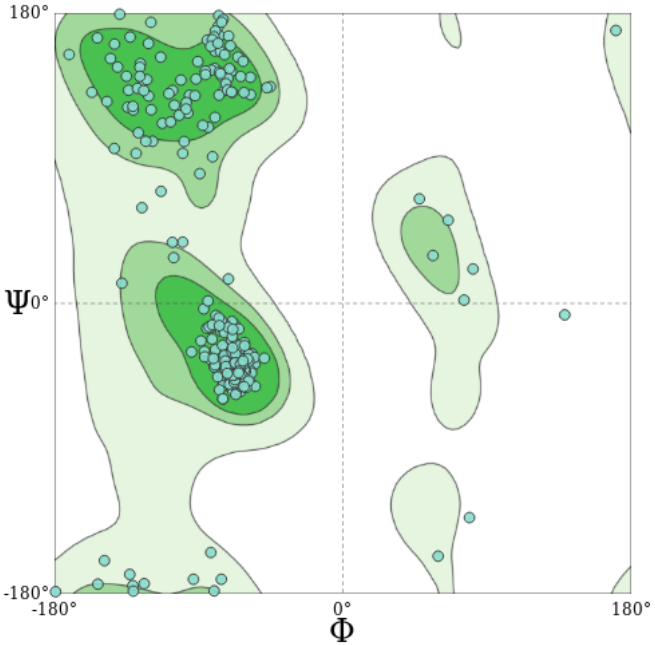

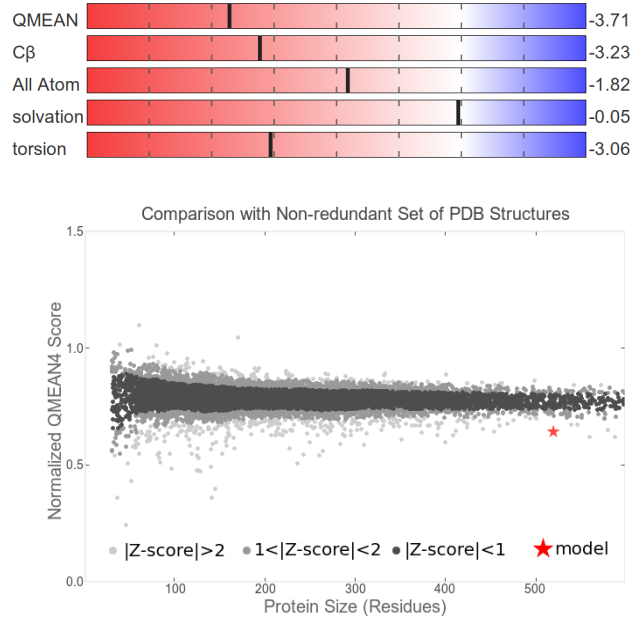

HORSE ACE2

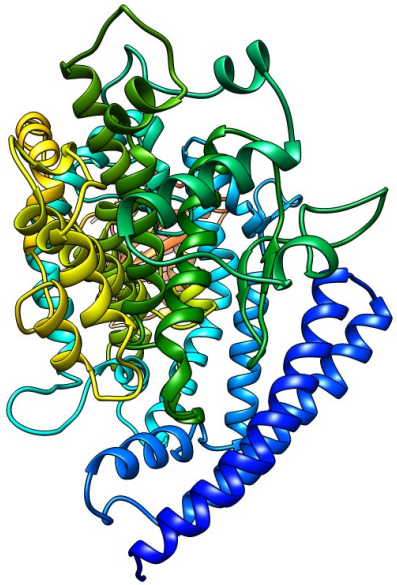

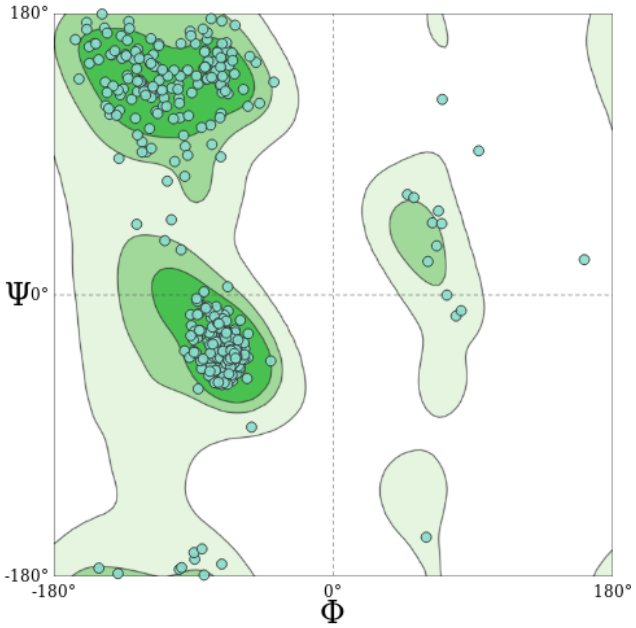

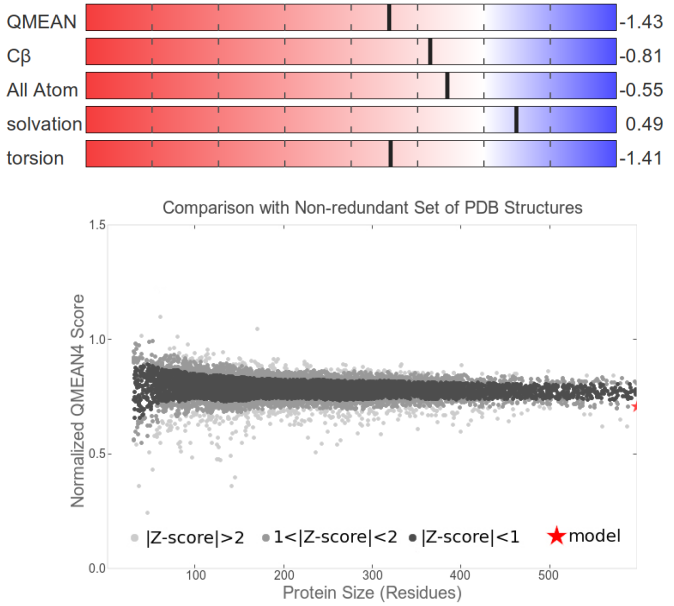

CATTLE ACE2

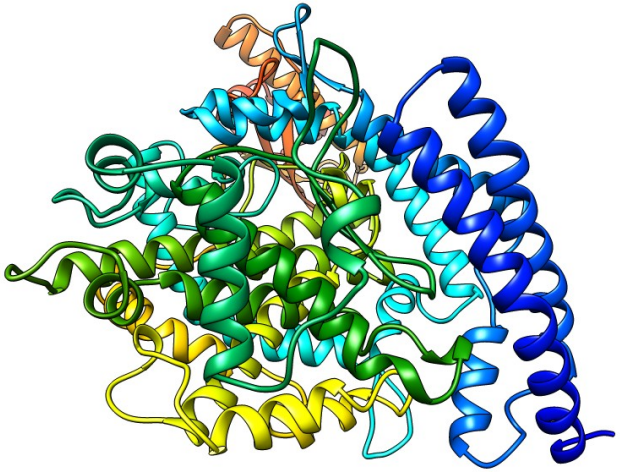

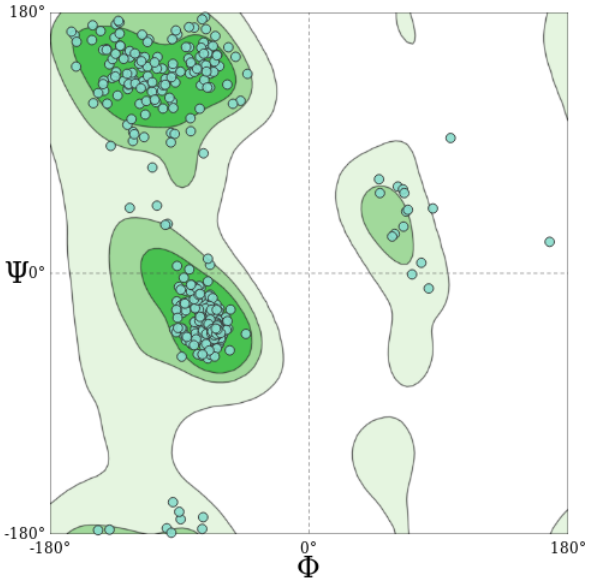

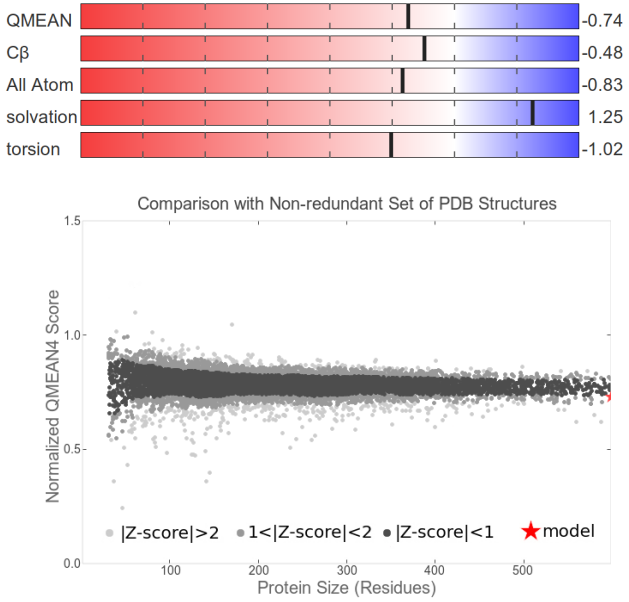

TIGER ACE2

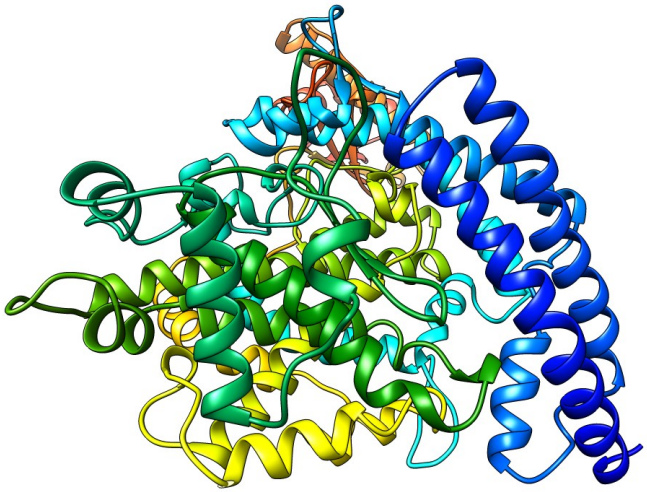

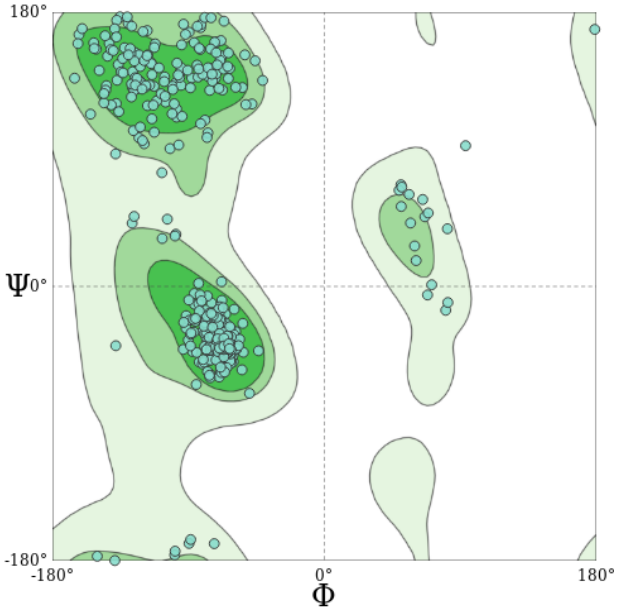

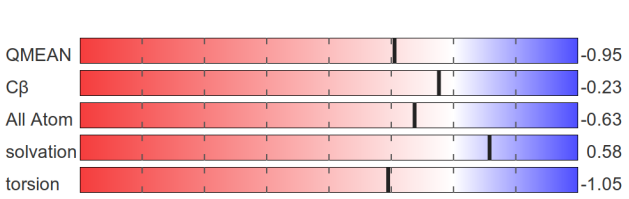

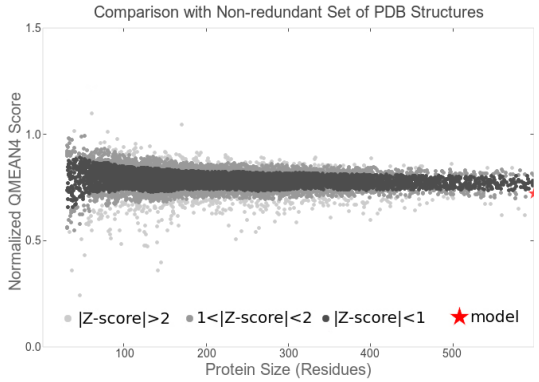

Supplementary Figure 3. Modelled ACE2 structures for selected species, with Ramachandran plots and quality met

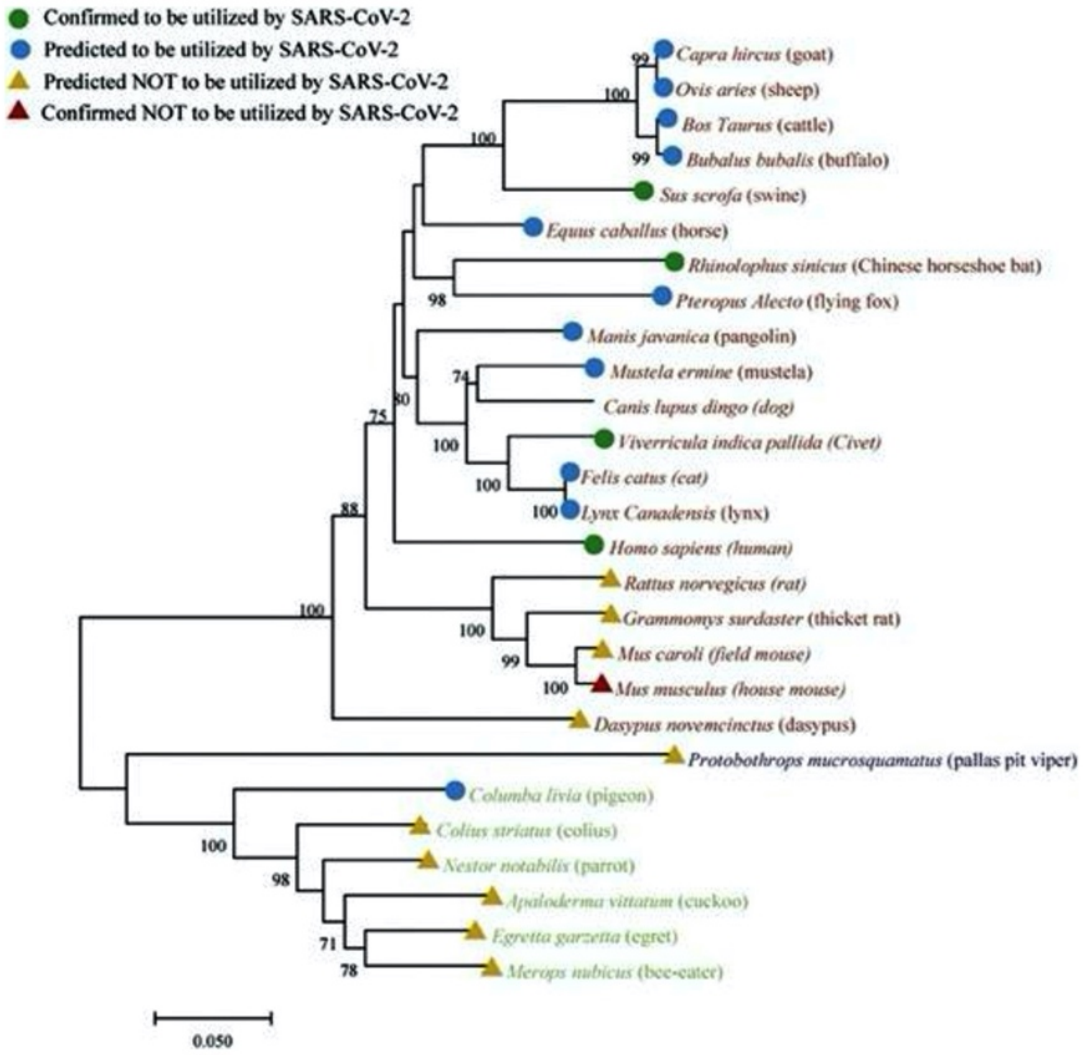

Supplementary Figure 4. Predicted and confirmed utilization of ACE2 receptors by the SARS-Cov-2 spike protein based on sequence homology from Qui et al.[1]

References

1 Qiu, Y. *et al.* Predicting the angiotensin converting enzyme 2 (ACE2) utilizing capability as the receptor of SARS-CoV-2. *Microbes Infect.* **22**, 221-225, doi:10.1016/j.micinf.2020.03.003 (2020).